Ecological Indicators 172 (2025) 113329

Contents lists available at ScienceDirect

Ecological Indicators

journal homepage: www.elsevier.com/locate/ecolind

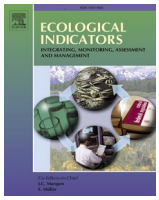

Coastal sediments record decades of cultural eutrophication in Tampa Bay, Florida, USA

Amanda R. Chappel [a,*], William F. Kenney [b], Matthew N. Waters [c], Caroline Buchanan Fisher [d], João H.F. Amaral [e], Edward J. Phlips [f], Elise S. Morrison [a,*]

[a] Engineering School of Sustainable Infrastructure and Environment, University of Florida, Gainesville, FL, USA
[b] Land Use and Environmental Change Institute, University of Florida, Gainesville, FL, USA
[c] Department of Crop, Soil, and Environmental Sciences, Auburn University, Auburn, AL, USA
[d] Department of Soil, Water, and Ecosystem Sciences, University of Florida, Gainesville, FL, USA
[e] Earth System Science Program, Faculty of Natural Sciences, Universidad del Rosario, Bogota, Colombia, USA
[f] School of Forest, Fisheries, and Geomatics Sciences, University of Florida, Gainesville, FL, USA

ARTICLE INFO

Keywords:
Cultural eutrophication
Estuarine biogeochemistry
Legacy nutrients
Phosphogypsum
Phosphorus sustainability
Radioisotopes
Sediment accumulation rates

ABSTRACT

Phosphorus (P) sustainability is a complex problem – it is a limited resource critical for agricultural productivity, but fertilizer production generates extensive phosphogypsum waste and can impair downstream water quality. Industrial, urban, and agricultural activities contribute to cultural eutrophication, thereby degrading both coastal and inland ecosystems and storing legacy nutrients in sediments. This study investigated the long-term effects of phosphogypsum wastewater discharges on legacy nutrient accumulation, an unintended impact of the fertilizer industry that is often overlooked and understudied. Sediment cores were collected to reconstruct the depositional history of two sites in Tampa Bay, Florida, USA that experienced past wastewater releases; the most recent in 2021. Sediments had high concentrations of stored or legacy nutrients (total P: 0.11 – 15.01 mg g^{-1}; total nitrogen: 0.04 – 0.37 %) particularly during discharge timeframes, as assessed by short-lived radioisotopes, and were predominantly in bioavailable forms, as assessed by bulk pools and ^{31}P nuclear magnetic resonance spectroscopy. These values are comparable to hypereutrophic lakes impacted by agriculture and urbanization. Sediment accumulation rates were elevated relative to other Florida estuaries (Bishop Harbor: 13,092 – 46,706 g m^{-2} yr^{-1}; Piney Point Creek: 3,064 – 23,990 g m^{-2} yr^{-1}), which can alter biogeochemical cycling and the fate of nutrient loading. Phosphorus accumulation rates and other proxies had downcore peaks corresponding to discharge events from 2001 to 2004, 2011, and 2021 with P accumulation rates ranging from 0.5 – 559 g m^{-2} yr^{-1}. These findings indicate that estuarine nutrient budgets need to incorporate stored sedimentary nutrient pools and internal benthic fluxes and highlight the need for a more sustainable P supply chain.

1. Introduction

To meet the global demand for agricultural production, phosphate mining and fertilizer production have led to a "broken biogeochemical cycle" of phosphorus (P) driven by a unidirectional flow from geological reserves to downstream aquatic systems (Elser and Bennett, 2011). Many efforts to manage P focus on improving agricultural practices, however, the byproducts of industrial fertilizer production can also negatively affect the environment. Globally, 300 million tons of phosphogypsum (PG), a byproduct of fertilizer production, is generated annually (Bilal et al., 2023). Rather than being reprocessed, the bulk of PG is stored long-term in constructed reservoirs (i.e., stacks) with finite lifespans, which are susceptible to structural failures (Beck et al., 2022, 2018; Pérez-López et al., 2016; Zielinski et al., 2011). Globally, about 28 % of PG is discharged to coastal waters (Bilal et al., 2023; Bouargane et al., 2023; Qin et al., 2023; Rutherford et al., 1994), where it can impair aquatic critical zones, emphasizing the need for a circular P economy that reduces waste and increases reuse (Bilal et al., 2023). This study evaluated the effects of PG discharge on estuarine sediments, which can act as reservoirs for nutrients, to determine how historical wastewater releases alter sediment and nutrient accumulation rates.

Phosphogypsum stack failures introduce high nutrient loads to

* Corresponding authors.
E-mail addresses: chappela@ufl.edu (A.R. Chappel), elise.morrison@essie.ufl.edu (E.S. Morrison).

https://doi.org/10.1016/j.ecolind.2025.113329
Received 14 November 2024; Received in revised form 6 March 2025; Accepted 6 March 2025
Available online 12 March 2025

coastal waters often as large pulse events. Cultural eutrophication (Malone and Newton, 2020; Smith, 1998) events such as these lead to harmful algal bloom (HAB) events (phytoplankton and macroalgae) in coastal areas, and associated ecosystem disruptions, such as seagrass loss, exposure to algal toxins, hypoxia, and aquatic animal mortalities (Garrett et al., 2011; Switzer et al., 2011; Beck et al., 2022; Morrison et al., 2023; Chen et al., 2023; Scolaro et al., 2023; Peñuelas and Sardans, 2022; Phlips et al., 2021). In addition to altering water column nutrients, PG wastewater contributes excess nutrients, contaminants, and radionuclides to sediments (Beck et al., 2022, 2018; Burnett and Elzerman, 2001; Gwynn et al., 2024; Morrison et al., 2023), thereby altering biogeochemical cycles and natural sedimentary processes within the impacted aquatic systems. Sediments are the ultimate sink of pollutants (Ardila et al., 2023; Rangel-Buitrago et al., 2023; Robledo Ardila et al., 2024; Törnquist et al., 2023) and enhanced loading of wastewater can alter sedimentation rates (Baskaran et al., 2014), sediment redox chemistry and remineralization (Corbett, 2010), and the storage of legacy nutrients (Niemitz et al., 2013). Recently, an important distinction has been made between the use of "legacy" and "residual" phosphorus. Here, we intentionally use the term "legacy nutrients" as we investigated the effects of anthropogenic nutrient discharges along the terrestrial-aquatic continuum (Zhou and Margenot, 2023). This study focused on how PG discharges alter estuarine sedimentation rates because changes in sedimentation rates are closely linked to biogeochemical cycling, nutrient storage, and the fate of external nutrient loading (Brenner et al., 2004; Foucher et al., 2021; Last et al., 2001; Schelske et al., 1994; Törnquist et al., 2023; Waters et al., 2019).

Since benthic-pelagic coupling is a primary driver of biogeochemical cycling in estuaries (Crump et al., 2023) and sediments are an important P source to coastal waters (Liu et al., 2020), sediments are a vital compartment for estuarine nutrient budgets and management strategies. In addition to the external nutrient loads of an estuary, sediments represent a potential source of internal nutrient loading, resulting in a new source of nutrients to the overlying water column (Carlson and Yarbro, 2006), which are frequently overlooked in aquatic ecological studies. The remobilization of legacy nutrients and contaminants stored in aquatic sediments contributes to eutrophication and will be further exacerbated by continued anthropogenic activities, climate change, and sea-level rise (Dellapenna et al., 2020; Gwynn et al., 2024; Niemitz et al., 2013). These persistent stressors coupled with growing coastal urbanization will make the current strategy for meeting pollution reduction targets with Total Maximum Daily Loads (TMDLs) difficult to achieve if confounding factors including the settling and resuspension of particle-bound nutrients and bioavailable nutrient regeneration are not properly accounted for (Lebo et al., 2012).

Progressive changes in the rate of cultural eutrophication and pollutant loads lead to adverse regime shifts that alter the fundamental structure and function of coastal ecosystems and are persistent and difficult to reverse (McGlathery et al., 2023; Phlips et al., 2021). This is particularly true for systems with extensive historic nutrient loading and storage of legacy nutrients (Niemitz et al., 2013; Rodgers et al., 2020). Because P and nitrogen (N)-driven eutrophication in aquatic ecosystems is increasing globally and exacerbates phenomena like coastal hypoxia (Carpenter and Bennett, 2011; Da et al., 2018) and dead zones (Altieri and Gedan, 2015; Diaz and Rosenberg, 2008), accounting for sediments in nutrient budgets and management plans is essential. Although estuarine restoration efforts have been increasingly successful, such as in Tampa Bay, Florida (DeAngelis et al., 2020), continued adaptive management strategies are needed to mitigate water quality and coastal habitat declines.

A recent event in the Tampa Bay Estuary (Florida, USA) highlights the importance of anthropogenic contributions to estuarine nutrient

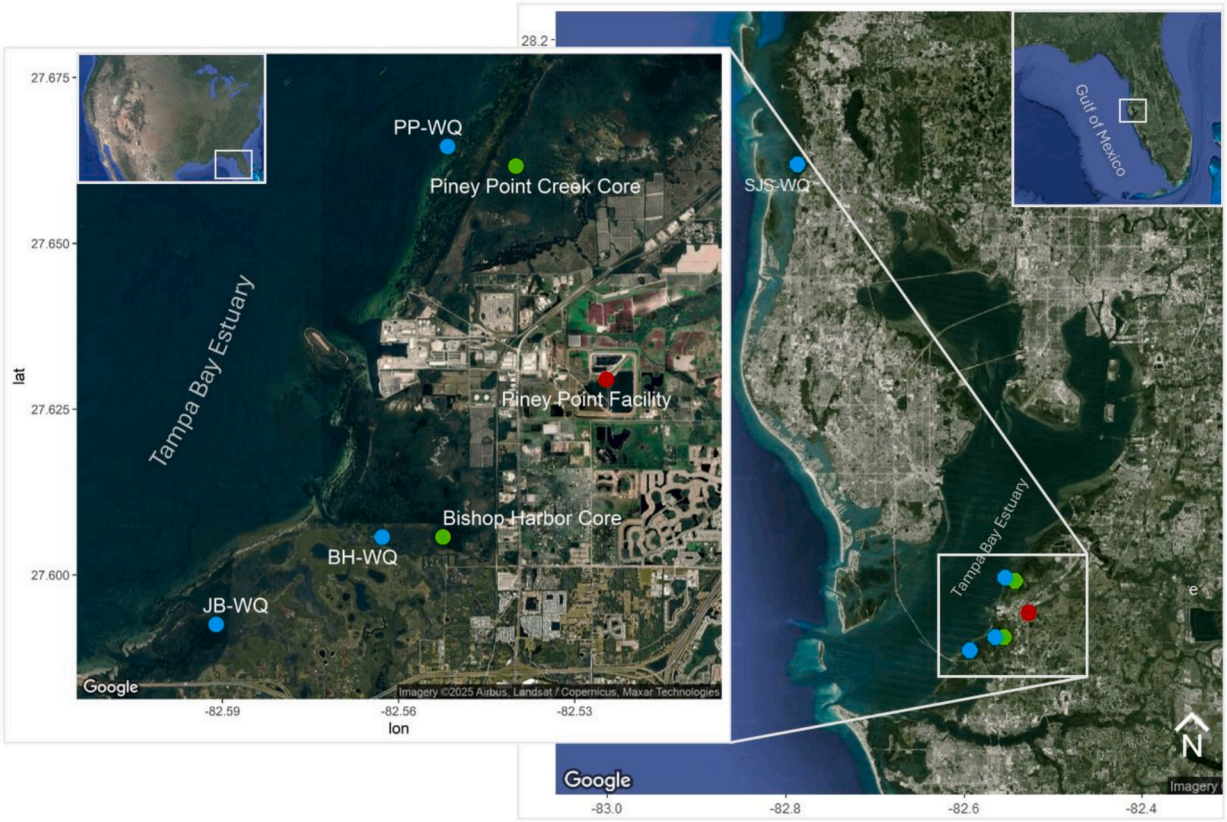

Fig. 1. Site Map of the Tampa Bay Estuary. The Tampa Bay estuary is located on the west coast of Florida, USA. Green points are sediment coring sites, blue points are water quality (WQ) sites, and the red point is the Piney Point Facility. PP = Piney Point; BH = Bishop Harbor; JB = Joe Bay; SJS = St. Joseph Sound. The site map was developed in R 4.2.2. (Kahle and Wickham, 2013) with visualization support by © Google Earth.

budgets. In 2021, 814 million L of high-nutrient effluent were released into the Bay from a PG storage facility through superficial outfalls (Beck et al., 2022; Chen et al., 2023; Morrison et al., 2023). The Piney Point facility, which sits on the coastal edge of Tampa Bay (Fig. 1), is a decommissioned fertilizer plant that operated from 1965 to 1996, when it transitioned solely into a PG storage facility (Henderson, 2004). The material at this facility is made up largely of gypsum ($CaSO_4{\cdot}2H_2O$), a solid byproduct that has a high affinity to bind with nutrients and contaminants (Rutherford et al., 1994; Silva et al., 2022). The PG is stored wet in acidic process waters high in nutrients, predominately diammonium phosphate, $(NH_4)_2HPO_4$, which remain from the fertilizer manufacturing process (Silva et al., 2022; Switzer et al., 2011). In addition to macronutrients, the pollutants of most environmental concern include radionuclides from the ^{238}Uranium decay series, fluoride, total dissolved solids, and complex sulfates (Rutherford et al., 1994). Previously, this PG stack suffered multiple structural failures and exceeded its holding capacity, requiring emergency releases of high-nutrient wastewater directly into Tampa Bay, most notably in 2001 – 2004, 2011, and 2021 (Beck et al., 2022; Garrett et al., 2011; Switzer et al., 2011). These historical discharges affected water column processes, but the long-term effects are not known.

This study investigated if, and to what magnitude, anthropogenic discharge events altered sediment and nutrient accumulation rates in the estuary by reconstructing the environmental history with radionuclides, stable isotopes, and bulk nutrients. Sediment cores were collected at two sites: Piney Point Creek, which was the location of the 2021 discharge event, and Bishop Harbor, which was a site of multiple discharges prior to 2021. Additionally, during the study period, Hurricane Ian (September 2022) caused retreating tides, reverse storm surge, and below-normal water levels, affording the opportunity to assess sediment and nutrient resuspension before and after the storm. This paper highlights the need to account for legacy nutrients when setting pollution reduction targets as well as the environmental impacts associated with past industrial releases that create nutrient imbalances in aquatic systems. Furthermore, there is an urgency to develop a sustainable circular P economy and improve PG recycling, when possible, to minimize future environmental impacts.

2. Materials and methods

2.1. Site Description

Two study sites were chosen along the eastern shoreline of lower Tampa Bay near the historic discharge locations of the Piney Point phosphogypsum facility, which has experienced multiple structural failures and has historically exceeded its holding capacity capabilities following storm events (Fig. 1). The study sites were co-located with long-term water quality monitoring sites presented in Morrison et al. (2023), which were established in consultation with the Tampa Bay Estuary Program and the University of South Florida's Tampa Bay Coastal Ocean Model (Chen et al., 2019, 2018; Liu et al., 2024). The sites included one site within Piney Point Creek, a tidal creek that connects the northern Piney Point discharge canal to Tampa Bay proper (Piney Point Creek), and one site within Bishop Harbor, a subbasin of lower Tampa Bay that connects the southern Piney Point discharge canal to Tampa Bay proper (Bishop Harbor; Fig. 1). During historic discharge events, wastewater effluent from the facility was released from the Piney Point Facility directly to the Tampa Bay estuary near these sampling locations through culverts and drainage ditches. The lead-210 (^{210}Pb) inventory at both sites exceeded the atmospheric fallout (Baskaran et al., 1993; Graustein and Turekian, 1986) suggesting these coring locations are sedimentation-focusing sites (e.g., depositional zones) where relatively preserved sediment records represent this nearshore environment.

2.2. Sample collection and Processing

One sediment core was collected from each study site in February 2022, two cores in total. Sediment cores were retrieved with a sediment–water interface piston corer (otherwise known as a Fisher Corer; Curtis et al., 1996; Fisher et al., 1992). The corer was driven into the seafloor until refusal, yielding a 45- and 51-cm compaction-free core at Bishop Harbor and Piney Point Creek, respectively. Both coring locations were devoid of submerged aquatic vegetation with patchy seagrass beds adjacent. Sediment cores were transported upright, stored in a cold room at 4° C overnight, and processed the day after collection with a core extruder. Cores were sectioned in one-centimeter intervals for the top 15 cm, then in two-centimeter intervals for the remaining base intervals. Samples (Bishop Harbor: n = 30, Piney Point Creek: n = 33) were then frozen and freeze-dried to obtain dry weight and dry bulk density downcore. Dried samples were homogenized and subsampled for subsequent analysis.

2.3. Radiometric Dating, Age-Depth Model, and rate Calculations

By using short-lived radionuclides as sediment proxies, which often behave similarly to pollutants of interest (Swarzenski et al., 2003), geochronologies of two cores were established to reconstruct the sedimentation record. An age-depth model was then applied to the radionuclide activity to calculate estimated changes in sedimentation rates over the past century (Appleby, 2008; Appleby and Oldfield, 1978; Last et al., 2001). Sediment deposition age and accumulation rates were determined using excess ^{210}Pb ($^{210}Pb_{Xs}$; e.g., Total ^{210}Pb – ^{226}Radium) a radioisotope that follows an exponential decay characterized by a half-life of 22.3 years. This decay rate makes it possible to calculate age and sedimentation rates for the past 100–150 years (Goldberg, 1963).

Freeze-dried homogenized sediment from each interval was packed in gamma tubes, sealed with epoxy, and set aside for 21 days to allow for ^{222}Radon to in-grow and establish secular equilibrium between ^{226}Ra and ^{214}lead/^{214}bismuth (^{214}Pb/^{214}Bi; Appleby and Oldfield, 1978; Smoak et al., 2013). Once secular equilibrium was reached, radioisotope activities were measured by low-background gamma detection using an intrinsic germanium well detector coupled to a multichannel analyzer (Ortec Well Detectors coupled with Ortec Maestro-32 Software Version 6.06; Kenney et al., 2022; Schelske et al., 1994) at the University of Florida's Gamma Spectroscopy Laboratory. Activity for ^{210}Pb was measured by the 46.5 KeV peak and ^{226}Ra (e.g., supported ^{210}Pb that forms in *situ* by using the gamma-emitting daughters ^{214}Pb and ^{214}Bi) at the 295.3, 351.9, and 609.3 KeV peaks (Schelske et al., 1994). Inventories of $^{210}Pb_{Xs}$ (dpm cm^{-2}) were calculated as the summation of the products of dry bulk density (DBD; g cc^{-1}) and $^{210}Pb_{Xs}$ activity (dpm g^{-1}) for all sediment sections in both cores (**Supplemental Information Table 1**).

The Constant Flux Constant Sedimentation-Constant Rate of Supply (CFCS-CRS) hybrid dating model was used to determine the time of deposition (sediment age) and sediment and nutrient accumulation rates. This model was used because these sites were in an estuary that is subject to both hurricane and episodic discharge events from Piney Point (Kenney et al., 2022; Krishnaswamy et al., 1971). Excess and supported thorium-234 (^{234}Th), and beryllium-7 (^{7}Be) were measured in the top six centimeters of both cores to determine whether a surface-mixed layer (SML) was present from bioturbation and/or physical mixing. Additionally, a biodiffusive mixing model was applied to the $^{210}Pb_{Xs}$ activity to further examine if a SML was present (Dellapenna et al., 1998). Due to a variable $^{210}Pb_{Xs}$ decay curve in the top portion of these cores, the age-depth model and associated interpretations were cautiously approached (Arias-Ortiz et al., 2018). The CFCS-CRS hybrid radiometric age-depth and biodiffusive mixing models were conducted using the Microsoft© Excel Solver Add-in. The mathematical approach and formulas used to determine activity at time of deposition and estimate sediment accumulation rates can be found in **Supplemental Information**.

2.4. Nutrient and stable isotopic analysis

Freeze-dried homogenized sediment from each interval was weighed into tin capsules for the analysis of elemental carbon (total [TC] and organic C[OC]) and total N (TN) and stable isotopes of C and N ($\delta^{13}C$ and $\delta^{15}N$). To avoid the confounding influence of inorganic C during the determination of the isotopic signature of OC, all carbonates were removed through acid fumigation to acquire representative OC and $\delta^{13}C$ values (Harris et al., 2001). Samples were analyzed at the University of Florida's Stable Isotope Laboratory on a Carlo Erba 1500 CN elemental analyzer coupled to a Thermo Electron Delta V Advantage isotope ratio mass spectrometer (Carlo Erba/ThermoFisher Scientific™, Waltham, MA, United States). Stable isotope ratios are reported for $\delta^{13}C$ and $\delta^{15}N$ in standard permil delta notation (‰) relative to Vienna Pee Dee Belemnite and atmospheric N_2 standards, respectively (Table 1). Analytical precision for C, N, and stable isotopes was calculated as the standard deviation of all standards analyzed during sample runs ($n = 18$), all of which were below acceptable error. Total C, OC, and TN are reported as mass percent (**Supplemental Information Table 3**), and the C:N, C:P, and N:P ratios are reported as mass ratios (Table 1).

The concentrations of total P, calcium (Ca), sulfur (S), iron (Fe), aluminum (Al), magnesium (Mg), and manganese (Mn; **Supplemental Information Table 3**) were analyzed for each interval by Inductively Coupled Plasma Atomic Emission Spectroscopy (ICP-AES) by the Waters Agricultural Laboratories, Inc (Camilla, GA). Samples were acid digested following EPA Method 3050B. This method is a digestion method for "environmentally available" elements that do not normally include elements bound to silicate structures. North American Proficiency Testing (NAPT) Program standards were used throughout each run to ensure analytical precision and duplicates were run every 22 samples to ensure reproducibility. Total Kjeldahl N (TKN) was analyzed for every other sediment interval by semi-automated colorimetry by the University of Florida's Analytical Research Laboratory (ARL; Gainesville, FL; National Environmental Laboratory Accreditation Program Certification-E72850). Samples were acid digested following EPA Method 351.2. All samples met precision limits of < 10 % and accuracy criteria of ± 10 %.

2.5. Phosphorus nuclear magnetic resonance spectroscopy

To evaluate the inorganic and organic P functional groups within the sediment cores, solution nuclear magnetic resonance spectroscopy for phosphorus (^{31}P NMR) was conducted on a subset of core intervals. Freeze-dried homogenized samples were extracted with a 1:20 solid-to-solution ratio of sodium hydroxide-disodium ethylenediaminetetraacetic acid (0.25 M NaOH – 0.05 M Na_2EDTA) for 16 h to maximize recovery of P due to the samples being high in calcium carbonate, iron, and aluminum, while increasing spectra resolution by removing paramagnetic metal ions (Buchanan Fisher et al., In Review; Cade-Menun and Liu, 2014; Xu et al., 2012; Cheesman et al., 2015; SFWMD et al., 2017). It is important to note that this alkaline extraction often accounts for approximately 30 – 60 % of TP (Cheesman et al., 2014; McLaren et al., 2015; Reddy et al., 2020), and may be lower in estuary sediments (Li et al., 2015; Watson et al., 2018). Following the NaOH-Na_2EDTA extraction, samples were centrifuged, decanted, and freeze-dried for 24 – 48 h. On the day NMR analysis was completed, the sample was combined with 1 M NaOH – 0.1 M Na_2EDTA, deuterium oxide (signal lock for the spectrometer), and metylendiphosphonic acid-P,P′-disodium salt (MDP; internal standard, $\delta = 17.46$ ppm). The sample solution was centrifuged and 500 μL was added to a 5 mm NMR ampule prior to

Table 1
Total phosphorus (TP), stochiometric nutrient ratios (mass ratios of carbon (C), nitrogen (N), and P), and stable isotopic ratios of C ($\delta^{13}C$) and N ($\delta^{15}N$).

Bishop Harbor							Piney Point Creek						
Depth (cm)	TP (mg g^{-1})	C:N	C:P	N:P	$\delta^{13}C$ (‰)	$\delta^{15}N$ (‰)	Depth (cm)	TP (mg g^{-1})	C:N	C:P	N:P	$\delta^{13}C$ (‰)	$\delta^{15}N$ (‰)
1	8.19	10.29	1.76	0.17	−22.94	0.58	1	0.56	13.16	66.01	6.65	−26.04	0.79
2	8.87	13.22	1.34	0.10	−23.11	1.08	2	0.42	20.33	91.67	7.14	−26.72	1.04
3	8.74	8.33	0.86	0.10	−22.73	1.15	3	0.30	13.93	69.44	4.98	−26.56	1.05
4	8.85	9.63	0.87	0.09	−22.76	1.18	4	0.30	16.06	86.24	5.37	−26.67	0.71
5	9.75	10.67	0.98	0.09	−22.44	1.23	5	0.27	12.31	72.69	5.90	−26.82	0.96
6	8.91	8.64	1.07	0.12	−22.65	1.36	6	0.23	13.21	81.86	6.19	−26.54	0.99
7	9.06	9.45	1.15	0.12	−22.60	1.50	7	0.21	10.22	89.76	8.78	−26.61	1.47
8	9.30	10.27	1.22	0.12	−22.55	1.40	8	0.23	9.39	73.48	7.83	−26.43	1.21
9	10.23	10.13	0.79	0.08	−22.36	1.54	9	0.30	12.36	89.77	7.26	−26.26	1.27
10	10.59	10.00	0.66	0.07	−22.37	2.02	10	0.30	11.58	120.88	10.44	−26.49	1.34
11	12.01	8.50	0.71	0.08	−21.97	1.79	11	0.35	15.37	140.86	10.00	−26.86	1.15
12	10.99	12.25	0.89	0.07	−21.86	1.90	12	0.29	10.00	96.55	9.66	−26.97	1.28
13	11.06	9.29	0.59	0.06	−22.01	2.34	13	0.31	15.00	86.26	5.75	−26.97	1.49
14	10.73	11.00	0.61	0.06	−21.98	2.23	14	0.30	14.58	92.64	6.35	−26.99	1.38
15	11.25	11.50	0.61	0.05	−22.00	2.42	15	0.26	10.42	104.23	10.00	−26.93	1.39
17	11.25	9.86	0.61	0.06	−22.03	2.11	17	0.33	18.29	95.11	5.20	−26.30	1.79
19	12.27	10.29	0.59	0.06	−21.54	2.35	19	0.39	15.57	56.48	3.63	−25.56	1.68
21	11.03	10.44	0.85	0.08	−21.47	2.46	21	0.33	12.78	70.77	5.54	−26.71	1.99
23	10.83	9.73	0.99	0.10	−21.52	2.52	23	0.28	11.79	59.78	5.07	−25.62	1.73
25	10.40	11.29	1.52	0.13	−21.33	2.34	25	0.30	10.77	47.30	4.39	−25.65	2.06
27	15.01	12.67	1.01	0.08	−20.91	2.76	27	0.25	15.82	62.75	4.45	−26.11	2.21
29	11.13	11.00	0.69	0.06	−20.57	2.34	29	0.21	13.75	52.13	3.79	−25.24	2.25
31	11.09	11.33	0.61	0.05	−20.32	2.42	31	0.21	13.00	43.54	3.35	−25.14	2.50
33	11.55	10.67	0.55	0.05	−20.49	2.52	33	0.22	9.29	29.95	3.23	−25.18	2.43
35	10.90	12.40	0.57	0.05	−20.37	2.45	35	0.23	12.50	21.93	1.75	−24.66	2.44
37	11.08	12.00	0.54	0.05	−20.55	2.46	37	0.14	7.80	28.26	3.62	−24.89	2.51
39	10.87	14.50	0.53	0.04	−20.08	2.34	39	0.20	13.33	20.51	1.54	−24.83	2.71
41	11.98	11.40	0.48	0.04	−19.81	1.05	41	0.14	10.67	22.38	2.10	−24.62	2.54
43	11.19	15.00	0.54	0.04	−19.45	2.45	43	0.15	9.00	11.84	1.32	−23.94	2.61
45	10.93	12.25	0.45	0.04	−19.44	2.11	45	0.18	10.00	11.24	1.12	−23.90	2.71
							47	0.21	13.00	12.56	0.97	−23.45	2.64
							49	0.12	10.00	16.67	1.67	−23.26	2.81
							51	0.11	12.00	22.02	1.83	−22.67	2.87
Mean	**10.67**	**10.93**	**0.82**	**0.08**	**−21.54**	**1.95**	**Mean**	**0.26**	**12.65**	**62.05**	**5.06**	**−25.68**	**1.82**
SE	**0.24**	**0.29**	**0.06**	**0.01**	**0.03**	**0.01**	**SE**	**0.02**	**0.48**	**6.00**	**0.49**	**0.03**	**0.01**

analysis on a Bruker Avance-III-600 spectrometer with a 5-mm BBO-Z probe at the McKnight Brain Institute at the University of Florida. Signals were assigned according to the literature (Buchanan Fisher et al., In Review; Cade-Menun, 2005; Makarov et al., 2002; Turner et al., 2003; SFWMD et al., 2017). Other acquisition details can be found in **Supplemental Information**.

2.6. Pre- and Post-Hurricane water column nutrients

On September 28, 2022, Hurricane Ian made landfall along the Gulf Coast of Florida (Saffir-Simpson Category 4) and resulted in a reverse storm surge in the study area (Heidarzadeh et al., 2023). Tampa Bay experienced a below-normal water level due to retreated tides and offshore wind coupled with 4 – 6 in. of rainfall (Bucci et al., 2023). Water samples were collected on September 26 and October 3, 2022, at long-term monitoring sites adjacent to the coring locations following methods from Morrison et al. (2023) and analyzed by the University of Florida's ARL. One site outside of Tampa Bay proper, St. Joseph Sound (SJS-WQ), was sampled as a control site and three sites were sampled in lower Tampa Bay: Bishop Harbor (BH-WQ), Piney Point (PP-WQ; both adjacent to sediment coring locations), and Joe Bay (JB-WQ; south of Bishop Harbor; Fig. 1). Water samples were collected and processed following EPA methods (**Supplemental Information**).

2.7. Data analysis

Summary statistics were calculated using Microsoft® Excel® for Microsoft 365 MSO (Version 2411, Build 16.0.18227.20082) and figures were constructed in R 4.2.2. (R Core Team, 2022) using tidyverse and ggplot2 packages (Wickham, 2016; Wickham et al., 2019).

3. Results

3.1. Radioisotope activities and Age-Date model

The CFCS-CRS hybrid dating model was used to calculate the date at a given depth, associated date range, and age of each sediment interval (**Supplemental Information Table 1**). The Bishop Harbor core (45 cm depth) captured a 31.6-year record (1990.5 – 2022.1 CE), while the Piney Point Creek Core (51 cm) captured a 96.4-year record (1925.7 – 2022.1 CE). The full ^{210}Pb inventory was not captured at the Bishop Harbor site, which was accounted for with the CFCS-CRS hybrid model yet resulted in a greater age error (5.9 – 16.4 years) for this core. In contrast, the full ^{210}Pb inventory was captured for the Piney Point Creek core, which resulted in lower age errors (1.9 – 7.6 years). Details of ^{210}Pb as a radioisotopic proxy and the associated age-depth model applied to these data are provided in **Supplemental Information**.

Total ^{210}Pb activity for Bishop Harbor averaged 5.3 dpm g^{-1} ± 0.1 (standard error) and 1.1 dpm g^{-1} ± 0.1 for Piney Point Creek (Fig. 2, **Supplemental Information Table 1**). Radium-226 activity (e.g., supported ^{210}Pb that forms in *situ*) was ~ 10-fold greater in the Bishop Harbor core with an average of 3.9 dpm g^{-1} ± 0.1 relative to the Piney Point Creek core average (0.4 dpm g^{-1} ± 0.02; Fig. 2, Table S1). The highest ^{226}Ra activity was measured in the surface interval of the Piney Point Creek core (1.1 dpm g^{-1} ± 0.1; activity error), which corresponded to 2021 ± 1.9 years (**Supplemental Information Table 1**). Except for the surface intervals (0 – 2 cm), ^{226}Ra activity did not exceed 0.56 dpm g^{-1} ± 0.1 over the last century at Piney Point Creek (Fig. 2, **Supplemental Information Table 1**) suggesting that this surface interval had ^{226}Ra inputs from an outside source, while Bishop Harbor had the highest ^{226}Ra activity around mid-depth (19 cm; 4.8 dpm g^{-1} ± 0.7) corresponding to 2011 ± 5.8 years (Fig. 2, **Supplemental Information Table 1**). Besides this peak at mid-depth, ^{226}Ra activity was relatively stable downcore at Bishop Harbor (**Supplemental Information Table 1**). Total ^{210}Pb and ^{226}Ra reached secular equilibrium in the Piney Point Creek core around 40 cm, whereas secular equilibrium was approached but not reached in the Bishop Harbor core, indicating that the full inventory was not captured (Fig. 2).

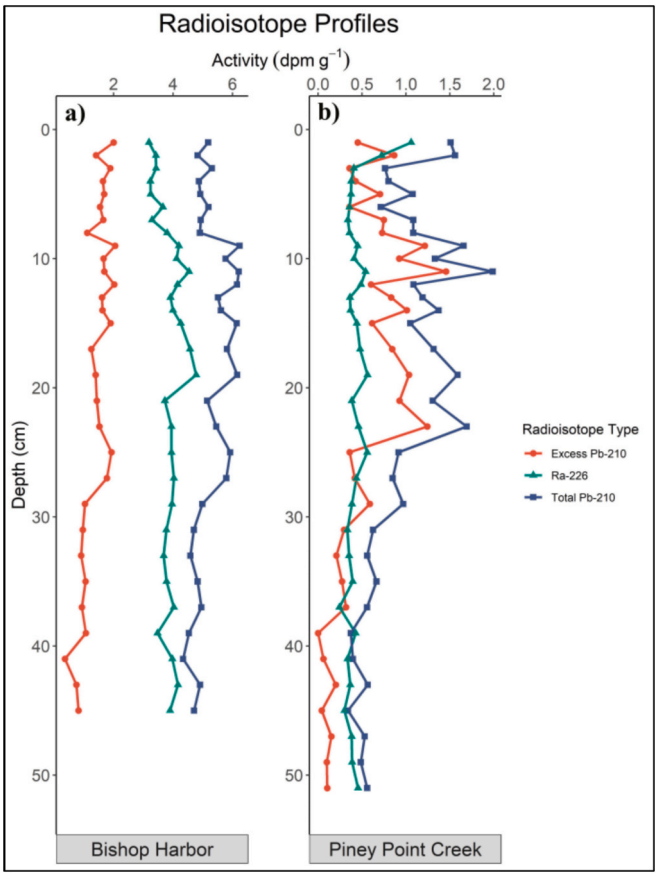

Fig. 2. The radioisotopic activity plotted as downcore profiles for Bishop Harbor and Piney Point Creek. Radioisotopic activity is presented in disintegrations per minute per gram (dpm g^{-1}) with X-axes on different scales for each plot and the Y-axes plotted as depth in centimeters (0 – 50 cm). Each profile includes the activity for total ^{210}lead (^{210}Pb; purple squares), excess ^{210}Pb (red circles), and ^{226}radium (^{226}Ra; green triangles) for a) Bishop Harbor and b) Piney Point Creek. Total ^{210}Pb reached secular equilibrium with ^{226}Ra in the Piney Point Creek core around 40 cm depth. The Bishop Harbor Core does not reach secular equilibrium, however, approaches it around 41 cm depth indicating that the full inventory was not captured for this site.

Excess ^{210}Pb activity averaged 1.4 dpm g^{-1} ± 0.1 and 0.6 dpm g^{-1} ± 0.1 for Bishop Harbor and Piney Point Creek, respectively (Fig. 2, **Supplemental Information Table 1**). The measured $^{210}Pb_{Xs}$ activity in both cores showed deviations from exponential decay in the top portion of the cores (top 25 cm for Bishop Harbor and top 23 cm for Piney Point Creek) that indicated varying sedimentation rates downcore. Sedimentation of allochthonous material can either enrich (e.g., PG discharge events) or dilute (e.g., hurricane and storm events) the radioisotope activity, both of which are captured in the top portion of these cores. Below these depths, the activity of $^{210}Pb_{Xs}$ decreased as a function of its half-life (Fig. 2). Excess and supported ^{234}Th and ^{7}Be were measured in the top six centimeters of both cores and had activities less than 1 dpm g^{-1} (**Supplemental Information Table 4**), indicating that minimal biological mixing occurred and was restricted to the top 5 cm and 3 cm for Bishop Harbor and Piney Point Creek, respectively.

3.2. Sediment and nutrient accumulation rates

Sediment accumulation rates (SAR) at Bishop Harbor represented the most recent ~ 31.6 years of depositional history and ranged from 13,092 – 46,706 g m^{-2} yr^{-1} with an average SAR of 20,454 g m^{-2} yr^{-1} ± 7,014

(standard error; Fig. 3, **Supplemental Information Table 2**). Within 0 – 2 cm depth a SAR of 24,297 g m^{-2} yr^{-1} was calculated corresponding with the 2021 Piney Point wastewater discharge event (Fig. 3). Elevated SARs were also identified at a depth of 15 – 17 cm (24,196 g m^{-2} yr^{-1}) and 29 – 33 cm (22,134 – 23,141 g m^{-2} yr^{-1}) that correspond with the 2011 and 2001 – 2004 Piney Point wastewater discharge timeframes, respectively (Fig. 3). Other elevated SARs include a rate of 32,893 g m^{-2} yr^{-1} at 8 cm depth, which was deposited between 2015.2 – 2021.3, which could be related to a storm event that increased runoff and sedimentation, or an undocumented anthropogenic source. Additionally, at 41 cm depth (1991.4 – 1995.6) Bishop Harbor had a twofold greater SAR (46,706 g m^{-2} yr^{-1}) than the cores average sedimentation rate (20,454 g m^{-2} yr^{-1} ± 7,014; Fig. 3). Further investigation is needed to determine the source(s) of these increased SARs during this timeframe.

Piney Point Creek had SARs that ranged from 3,064 – 23,990 g m^{-2} yr^{-1} with an average of 6,718 g m^{-2} yr^{-1} ± 448, representing the most recent ~ 96.4 years of depositional history at this site (Fig. 3, **Supplemental Information Table 2**). This site exhibited a ~ twofold increase in average SARs in the most recent decade (2012 – 2022; 10,310 g m^{-2} yr^{-1} ± 1,862) compared to the base of the core (1926–2012; 6,293 g m^{-2} yr^{-1} ± 487). The most recent decadal timeframe corresponds to the two most recent documented discharge events from Piney Point (2011 and 2021) that are likely responsible for skewing this decadal average. Other notable elevated SARs include those recorded at 6 cm (2018.1 – 2020.7), 41 cm (1953.4 – 1955.4), and 45 cm depths (1943.9 – 1945.9; Fig. 3), which do not correspond to documented Piney Point discharge events.

Total P and N accumulation rates (TPAR and TNAR) were also used to investigate nutrient storage potential and temporal changes at these sites. The TPAR for Bishop Harbor ranged from 136 – 559 g m^{-2} yr^{-1}, with an average of 230 g m^{-2} yr^{-1} ± 12 (Fig. 3, **Supplemental Information Table 2**). The most recent TPAR decadal average at Bishop Harbor was 234 g m^{-2} yr^{-1} ± 9, and surface intervals (0–2 cm) had a TPAR of 208 g m^{-2} yr^{-1} ± 30 corresponding to the 2021 discharge timeframe. Elevated TPARs were measured further downcore and corresponded to the 2011 (255 – 272 g m^{-2} yr^{-1}) and 2001 – 2004 (246 – 267 g m^{-2} yr^{-1}) discharge timeframes (Fig. 3). At 41 cm depth, Bishop Harbor's TPAR was 559 g m^{-2} yr^{-1}, which was almost three times greater than the downcore average and corresponds with the early 1990s (Fig. 3). Additional investigation is needed to determine the source(s) of TP in this interval. Piney Point Creek TPARs (0.5 – 10.8 g m^{-2} yr^{-1}) were an order of magnitude lower than those of Bishop Harbor, with an average of 1.5 g m^{-2} yr^{-1} ± 0.4 (Fig. 3, **Supplemental**

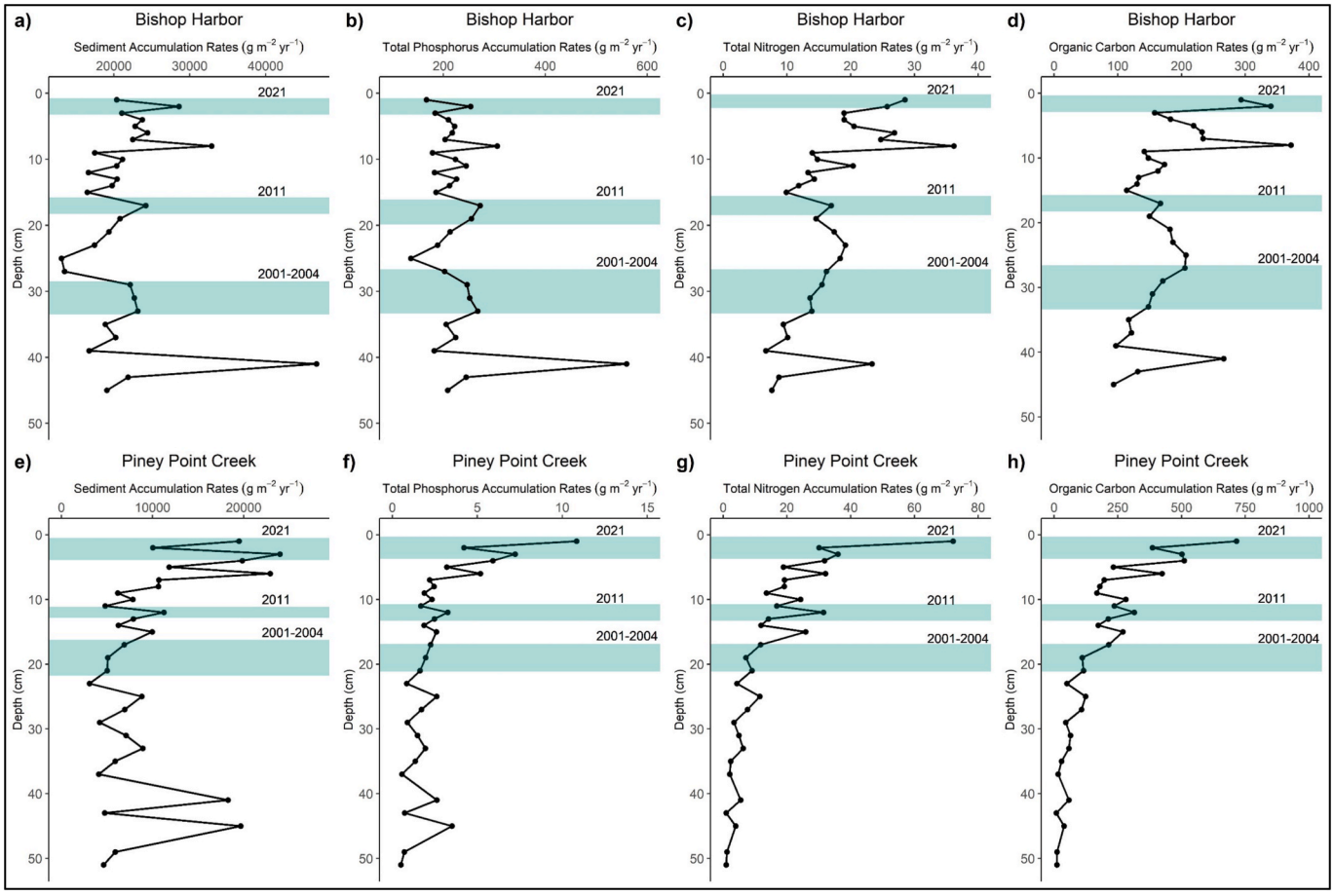

Fig. 3. Sediment and nutrient accumulation rates plotted as downcore profiles for Bishop Harbor (a – d) and Piney Point Creek (e – h). Rates are shown in grams per meter squared per year (g m^{-2} yr^{-1}) with X-axes on different scales for each plot and the Y-axes plotted as depth in centimeters (0 – 50 cm). The top figures represent downcore profiles of Bishop Harbor for a) sediment accumulation rates (SARs), b) total phosphorus accumulation rates (TPARs), c) total nitrogen accumulation rates (TNARs), and d) organic carbon accumulation rates (OCARs). The Bishop Harbor profiles represent a 31.6-year record (1990.5 – 2022.1 CE) captured with a 45-cm sediment core. The bottom figures represent the downcore profiles of Piney Point Creek for e) SARs, f) TPARs, g) TNARs, and h) OCARs. The Piney Point Creek profiles represent a 96.4-year record (1925.7 – 2022.1 CE) captured in a 51-cm sediment core. The green horizontal bars represent periods of historic wastewater releases from the Piney Point phosphogypsum facility (2021, 2011, and 2001 – 2004) determined from the age-depth model applied to the radioisotopic activity of each core. Elevated peaks at 41 and 45 cm depth in Fig. 3e correspond with the years 1953.4 – 1955.4 and 1943.9 – 1945.9, respectively, prior to the Piney Point Facility being established. The elevated peak at 41 cm depth in Fig. 3a – d corresponds to the year 1991.4 – 1995.6. Additional 5.4 research is needed to determine if this peak corresponds to a discharge event from the Piney Point facility or a different environmental or anthropogenic event.

Information Table 2). The most recent decadal average for TPARs at this site was 3.1 g m^{-2} yr^{-1} ± 0.7, suggesting increased TP accumulation since 2011. The surface interval of this core had a TPAR of 10.8 g m^{-2} yr^{-1}, corresponding to the 2021 discharge timeframe, and represents the maximum TPAR found in this core.

Bishop Harbor had TNAR that ranged from 6.7 – 36.2 g m^{-2} yr^{-1}, with an average of 15.2 g m^{-2} yr^{-1} ± 1.2 (Fig. 3, **Supplemental Information Table 2**). The most recent decadal TNARs averaged 19 g m^{-2} yr^{-1} ± 1.7, with the highest TN accumulation rates (36.2 g m^{-2} yr^{-1}) during the 2015.2 – 2021.3 timeframe. Additional investigation is needed to determine the source(s) of TN in this interval. Piney Point Creek TNARs ranged from 0.9 – 72.2 g m^{-2} yr^{-1}, with an average of 6.4 g m^{-2} yr^{-1} ± 2.6 (Fig. 3, **Supplemental Information Table 2**). The maximum TNAR (72. 2 g m^{-2} yr^{-1}) was measured in the surface interval, corresponding to the 2021 Piney Point discharge timeframe with the most recent decadal average (22.7 g m^{-2} yr^{-1} ± 4.1) being skewed greatly by the N deposited in this surface interval.

Organic C accumulation can act as a proxy for primary productivity and biogeochemical responses and provide insights into sediment redox conditions. It has been found that P enrichment can be inferred from changes in C accumulation within sediments (Schelske et al., 1988). Likewise, Waters et al. (2019) showed OC storage linked to eutrophic conditions in Florida lakes. Bishop Harbor had OC accumulation rates (OCAR) from 93 – 372 g m^{-2} yr^{-1}, with an average rate of 167 g m^{-2} yr^{-1} ± 12 (Fig. 3, **Supplemental Information Table 2**), and the most recent decade average was 192 g m^{-2} yr^{-1} ± 19, suggesting an increase in C deposition since 2011. However, further studies on early diagenetic processes in this estuary are needed to strengthen this inference. Organic C accumulation rates at Piney Point Creek ranged from 9 – 716 g m^{-2} yr^{-1}, with an average OCAR of 79.5 g m^{-2} yr^{-1} ± 30 and the most recent decadal average was 275 g m^{-2} yr^{-1} ± 44 (Fig. 3, **Supplemental Information Table 2**), likely representing increased C deposition over the most recent decade with an increase in eutrophication events. With the largest OCARs at both sites occurring within the surface intervals corresponding to the 2021 discharge event, we suggest that increased C accumulation is a direct reflection of these cultural eutrophication events.

3.3. Sediment nutrients and stable isotopes

Average TP concentrations downcore were two orders of magnitude greater at Bishop Harbor (10.67 mg g^{-1} ± 0.24; standard error) compared to Piney Point Creek (0.26 mg g^{-1} ± 0.2). Total P concentrations at Bishop Harbor ranged from 8.19 – 15.01 mg g^{-1}, with a general increase with depth (**Supplemental Information Fig. 1**, Table 1). TP concentrations at Bishop Harbor peaked between 25–27 cm depth (15.01 mg g^{-1}), corresponding to the 2001–2004 Piney Point discharge timeframe. Piney Point Creek TP concentrations ranged from 0.11 – 0.56 mg g^{-1} and generally decreased with depth (Table 1). The surface interval of the Piney Point Creek core had the highest TP concentration (0.56 mg g^{-1}), corresponding to the 2021 discharge timeframe from Piney Point.

Percent TN for Bishop Harbor averaged 0.08 % ± 0.02 and 0.14 % ± 0.02 for Piney Point Creek (**Supplemental Information Fig. 2 and Table 3**). The surface interval and 25 cm depth interval of Bishop Harbor had the greatest %TN values (0.14 %), while %TN was greatest in the surface interval (0.37 %) and at 11 cm depth (0.35 %) at Piney Point Creek. Depth intervals with the highest %TN values coincided with intervals associated with Piney Point discharge events, suggesting the deposition of N to the bedload. Total Kjeldahl N, the portion of TN that is ammonium (NH_4^+) and organic N, was found to represent the bulk of N in these samples with Bishop Harbor's averaging 0.07 % ± 0.02 and Piney Point Creek's averaging 0.12 % ± 0.02.

Percent TC for Bishop Harbor averaged 1.22 % ± 0.05 with an average %OC of 0.85 % ± 0.03 with the greatest %TC (2.27 %) and %OC (1.58 %) found at a depth of 25 cm corresponding to the 2001 – 2004 discharge timeframe (**Supplemental Information Table 3**). Percent TC for Piney Point Creek averaged 2.15 % ± 0.05 with an average %OC of 1.80 % ± 0.03 with the greatest %TC (4.99 %) and %OC (4.93 %) found at a depth of 11 cm corresponding to the 2011 discharge timeframe (**Supplemental Information Table 3**). These high C intervals coinciding with known Piney Point discharge timeframes suggest the deposition of C-rich suspended particulate material (SPM) from the facility or phytoplankton biomass following the discharge events or both (Chen et al., 2023; Morrison et al., 2023).

Macronutrient mass ratios including C:N, C:P, and N:P were calculated for both sites to assess changes in stoichiometry downcore (Table 1). At Bishop Harbor, C:N ranged from 8.3 – 15 with an average of 10.9 ± 0.3, C:P ranged from 0.5 – 1.8 with an average of 0.8 ± 0.1, and N:P ranged from 0.04 – 0.17 with an average of 0.08 ± 0.01 (Table 1). At Piney Point Creek, C:N ranged from 7.8 – 20.3 with an average of 12.6 ± 0.5, C:P ranged from 11.2 – 140.9 with an average of 62.1 ± 6.0, and N:P ranged from 1.0 – 10.4 with an average of 5.1 ± 0.5 (Table 1). When these nutrient ratios were compared between sites, C:N values had similar downcore trends, however, P concentrations skewed C:P and N:P ratios (Table 1).

The $\delta^{13}C$ values for both cores became enriched (more positive) with depth (**Supplemental Information Fig. 3**; Table 1). For Bishop Harbor, the $\delta^{13}C$ value within the surface interval was –22.94 ‰ which transitioned to −19.44 ‰ at depth (45 cm). For Piney Point Creek, the $\delta^{13}C$ value within the surface interval was −26.04 ‰ which transitioned to –22.67 ‰ at depth (51 cm). When $\delta^{13}C$ values were plotted against C:N ratios, the predominate endmembers contributing to these sediments include marine phytoplankton and particulate OC, freshwater plankton, and terrestrial C3 plants (**Supplemental Information Fig. 3**; Lamb et al., 2006; Morrison et al., 2023). Generally, $\delta^{15}N$ values became enriched with depth for both cores, however, $\delta^{15}N$ values showed a smaller difference between surface and base intervals when compared to $\delta^{13}C$ values (Table 1). For Bishop Harbor, the $\delta^{15}N$ values had a surface value of 0.58 ‰ and a base value of 2.11 ‰ at 45 cm depth. For Piney Point Creek, the $\delta^{15}N$ values had a surface value of 0.79 ‰ and a base value of 2.71 ‰ at 51 cm depth (Table 1).

Detailed values of sedimentary elements can be found in Fig. 4 and **Supplemental Information Table 3**. Of particular interest to this study were Ca, S, Fe, Al, Mg, and Mn as these elements have high concentrations in PG stacks including Piney Point (Burnett and Elzerman, 2001). At Bishop Harbor, Ca concentrations ranged from 25.90 – 44.68 mg g^{-1} with an average concentration of 31.9 mg g^{-1} ± 0.80. Sulfur concentrations at this site ranged from 2.16 – 5.720 mg g^{-1}, with an average concentration of 3.01 mg g^{-1} ± 0.14. Elevated concentrations of both Ca and S (two major components of PG, $CaSO_4{\cdot}2H_2O$) were highest at Bishop Harbor around 25 cm depth, corresponding to the 2001–2004 discharge timeframe from Piney Point. Calcium concentrations measured at Piney Point Creek ranged from 1.32 – 4.11 mg g^{-1}, with an average concentration of 2.31 m g^{-1} ± 0.12. Sulfur concentrations measured at Piney Point Creek ranged from 0.2987 – 3.65 mg g^{-1}, with an average concentration of 1.66 mg g^{-1} ± 0.15. The highest concentrations of Ca and S at Piney Point Creek were between 11 and 14 cm depth, corresponding to the 2011 discharge timeframe.

3.4. Phosphorus nuclear magnetic resonance spectroscopy

Phosphorus NMR was conducted at three sediment intervals for each site: a surface-depth interval (1–2 cm), a mid-depth interval (10–11 cm for Bishop Harbor, 14–15 cm for Piney Point Creek), and a base-depth interval (43–45 cm for Bishop Harbor, 21–23 cm for Piney Point Creek). Different core depths were used for the mid-and base depths of each core to ensure the intervals analyzed were from the same approximate sedimentation date. Results from ^{31}P NMR confirmed that most of the P in these samples was in the form of orthophosphate (orthoP), an inorganic form of P (**Supplemental Information Fig. 4**a–d). The one exception was Piney Point Creek 1 – 2 cm, which had a small peak of

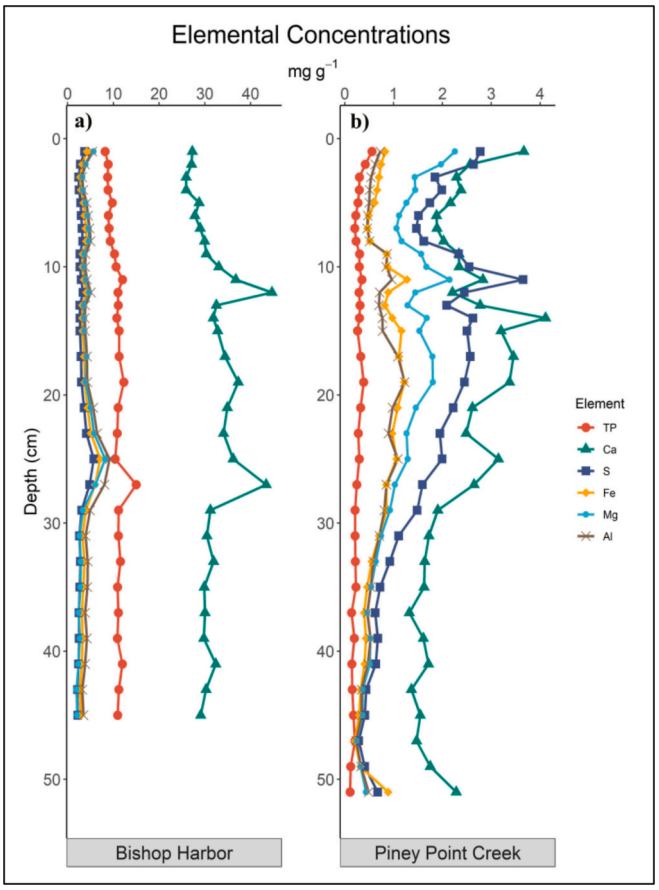

Fig. 4. Downcore profiles of elemental concentrations for Bishop Harbor (a) and Piney Point Creek (b). Elemental concentrations include total phosphorus (TP; red circles), calcium (Ca; green triangles), sulfur (S; purple squares), iron (Fe; orange diamond), magnesium (Mg; blue bullet), and aluminum (Al; brown cross) measured by Inductively Coupled Plasma Atomic Emission Spectroscopy (ICP-AES) presented in mg g^{-1}. These elements are all known to be in high concentrations in phosphogypsum including at the Piney Point Facility (Burnett and Elzerman, 2001).

pyrophosphate, an inorganic biogenic form of P. No organic forms of P were identified in any of the samples analyzed. To ensure that no other P compounds were muted by background noise on the NMR spectra, samples were re-analyzed following a pretreatment method according to Defforey et al. (2017). The resultant spectra from these samples were similar to the results from the initial ^{31}P NMR analysis (**Supplemental Fig. 4**b and d).

3.5. Pre- and Post-Hurricane water column nutrients

Storm-driven nutrient resuspension near the study sites was investigated using water column data collected before and after Hurricane Ian made landfall on the Gulf Coast of Florida (September 28, 2022). A control site outside of Tampa Bay (St. Joseph Sound) exhibited a net decrease in water column nutrients after Hurricane Ian, from 550 μg L^{-1} to 490 μg L^{-1} TKN, and from 4.81 μg L^{-1} to 1.8 μg L^{-1} orthoP, which could be attributed to a dilution effect from rainfall (Table 2; Jani et al., 2020). However, the three lower Tampa Bay sites exhibited increased water column nutrients after Hurricane Ian, with Bishop Harbor showing the greatest increase, from 410 μg L^{-1} to 920 μg L^{-1} TKN and 34.9 μg L^{-1} to 91.7 μg L^{-1} orthoP (Table 2). Joe Bay, another back bay region south of Bishop Harbor, showed a similar increase from 480 μg L^{-1} to 1060 μg L^{-1} TKN and 31.8 μg L^{-1} to 68.9 μg L^{-1} orthoP. Piney Point showed a smaller increase in TNK (520 μg L^{-1} to 610 μg L^{-1}) and orthoP (47.6 μg L^{-1} to 48.4 μg L^{-1}) compared to Bishop Harbor and Joe Bay. The SPM of the lower Tampa Bay sites had more enriched δ^{13}C values and more depleted δ^{15}N values after the passing of the hurricane. These observed increases in water column nutrients and shifts in stable isotope values could be a result of nutrients released from resuspended sediments (Corbett, 2010; Fadum et al., 2023; Paerl et al., 2018).

4. Discussion

4.1. Radioisotopes as proxies for altered sedimentation

The ^{226}Ra and ^{210}Pb provided insights into the most recent (2021) and historical (2011, 2001 – 2004) discharge events from the Piney Point PG facility. The highest activities of ^{226}Ra were seen at timeframes associated with direct discharges to each site: in the Piney Point Creek's surface interval (2021 ± 1.6 years) and mid-depths in the Bishop Harbor core (2011 ± 5.2 years; 2001 – 2004 ± 4.3 years). Because PG is high in radioisotopic activity, and Florida deposits are particularly rich in ^{226}Ra (Baskaran and Swarzenski, 2007; Burnett and Elzerman, 2001), it can be inferred that these sediment intervals captured past wastewater discharge events, lending insight into altered sedimentation rates during these periods. ^{226}Radium activities, especially for the Bishop Harbor core, were greater than those previously reported for other Florida estuaries (Javaruski et al., 2022; Robbins et al., 2000). Excess ^{210}Pb activity also suggested that the episodic wastewater events were recorded in the sediments, represented by variable decay curves in the top ~ 25 cm of the cores (Baskaran et al., 2014; Dellapenna et al., 1998; Swarzenski et al., 2006), where bulk homogenized material was deposited during PG discharge timeframes (Fig. 3). Beryllium-7 and ^{234}Th activities suggest bioturbation was constrained to the top 3–5 cm of both cores (Table S4). The ^{210}Pb and ^{226}Ra results differ from a recent study conducted in Tampa Bay (Larson et al., 2023), but the data indicate that Larson et al. (2023) did not collect depositional sediments.

Although we were not able to use an independent time marker (e.g., ^{137}Cesium) to validate the age-depth model (Kaste et al., 2021), the model was supported by other chemical markers abundant in PG and diammonium phosphate (Fig. 4, Table 1, and **Supplemental Information Table 3**). In particular, TP, TN, Ca, and S exhibited elevated concentrations during discharge timeframes, representing independent

Table 2
Nutrient concentrations were collected before (9/26/2022) and after Hurricane Ian (10/05/2022) made landfall on the Gulf Coast of Florida on September 28, 2022. Samples were collected from long-term water quality monitoring sites adjacent to sediment coring locations from Morrison et al. (2023). St Joseph Sound was the control site for this study and was located outside of Tampa Bay Proper. Nutrient acronyms: NH4 = ammonium, NOx = nitrate and nitrite species, TKN = total Kjeldahl nitrogen, OrthoP = orthophosphate. The stable isotopes of carbon (δ^{13}C) and nitrogen (δ^{15}N) were analyzed from suspended particulate material collected from the water column at these sites.

Site	ID	NH_4 (μg L^{-1})		NO_x (μg L^{-1})		TKN (μg L^{-1})		OrthoP (μg L^{-1})		δ^{13}C (‰)		δ^{15}N (‰)	
		Pre-Ian	Post-Ian	Pre-Ian	Post-Ian	Pre-Ian	Post-Ian	Pre-Ian	Post-Ian	Pre-Ian	Post-Ian	Pre-Ian	Post-Ian
St. Joseph Sound	SJS-WQ	0.08	0	0.07	0.04	550	490	4.81	1.78	−21.81	−23.00	3.67	1.03
Piney Point	PP-WQ	0.09	0	0.07	0.06	520	610	47.58	48.4	−24.27	−23.09	3.88	3.18
Bishop Harbor	BH-WQ	0.06	0	0.06	0.05	410	920	34.92	91.73	−23.72	−22.4	3.43	2.82
Joe Bay	JB-WQ	0.06	0	0.06	0.07	480	1060	31.76	68.88	−23.2	−21.83	1.67	2.46

chemical makers that corroborate the inferences made from the radioisotopic activity and the age-depth model (Fig. 4). Calcium displayed the highest concentrations and clearest peaks corresponding to the discharge events followed by S, both of which are major components of PG (Burnett and Elzerman, 2001; Rutherford et al., 1994).

4.2. Altered sedimentation relative to discharge events

Both study sites exhibited elevated SARs during the two most recent discharge timeframes from Piney Point (2021 and 2011; Fig. 3). Bishop Harbor also had elevated SARs during the 2001 – 2004 timeframe when releases were discharged directly to the back bay basin. The SARs were unexpected for these estuarine sediments because Tampa Bay had previously been identified as a particle-limited system (Baskaran and Swarzenski, 2007). Rates measured in this study (Bishop Harbor: 13,092 – 46,706 g m^{-2} yr^{-1}, Piney Point Creek: 3,064 – 23,990 g m^{-2} yr^{-1}) were mostly greater than those of other Florida estuaries that receive inputs from higher magnitude rivers than those draining into Tampa Bay, such as Estero Bay at the mouth of the Caloosahatchee River (300 – 11,100 g m^{-2} yr^{-1}; Javaruski et al., 2022) and Florida Bay south of the Florida Everglades (1,700 – 9,200 g m^{-2} yr^{-1}; Robbins et al., 2000). This indicates anthropogenic activity, including industrial discharge events, can alter sedimentation rates, which in turn can influence biogeochemical dynamics that drive benthic-pelagic coupling and ecosystem services. These sedimentation rates also suggest that effluent was transported from the 2021 discharge points to Bishop Harbor, supporting forecasts made by the Tampa Bay Coastal Ocean model (Liu et al., 2024).

The elevated TP and TN accumulation rates at these sites during wastewater discharge timeframes help explain where some portion of the discharged nutrients went (Fig. 3) and highlight how wastewater releases influence nutrient accumulation in estuarine sediments. High P concentrations were also found in surface sediments near these study sites collected by Major and Pasek (2024) following the 2021 Piney Point discharge event, corroborating that Piney Point contributed a portion of these nutrients to the sediments of the back bay regions of Tampa Bay. The nutrient accumulation rates indicate that these areas can store large quantities of legacy nutrients predominantly in the form of orthoP, as shown by ^{31}P NMR analysis, and NH_4^+, and organic N, as shown by bulk pool analysis. Because Tampa Bay is an N-limited system (Beck et al., 2022), these eutrophication events impaired estuarine water quality and ecosystem services (Beck et al., 2022; Chen et al., 2023; Garrett et al., 2011; Morrison et al., 2023; Scolaro et al., 2023; Switzer et al., 2011), with potential long-term effects of legacy nutrients in the future. Total P accumulation rates measured in this study are orders of magnitude greater than those measured in Green Bay, Lake Michigan (< 1 g m^{-2} yr^{-1}), a freshwater estuary that has been identified as an Area of Concern due to legacy nutrient pollution (Lin et al., 2024). These findings are also comparable to or greater than the P concentration of hypereutrophic lakes in Florida surrounded by intensive agriculture (Engstrom et al., 2006; Kenney et al., 2001). Although the sediment cores used in this study are not necessarily representative of nutrient storage and sedimentation dynamics of all regions of the Bay, they provide insights for regions of the bay where residence times and nutrient loading are of similar magnitude, such as protected back bay regions throughout middle and lower Tampa Bay, as well as portions of Old Tampa Bay.

With the exception of Piney Point discharge events, nutrient loads to Tampa Bay from the watershed as a whole have remained relatively constant from 1985 to 2021 (N loading between ~ 3,000 – 4,000 tons; Greening et al., 2014; Janicki Environmental Inc, 2023). However, water column TN and TP concentrations have declined, which has been attributed to decreased nutrient flux from sediments (Greening et al., 2014). This suggests that extreme nutrient-loading events that occurred before the 1980s (i.e., before point source pollution reduction efforts began) had a legacy effect on water quality well into the 21st century and highlight the potential for current cultural eutrophication events to have long-term effects. As we work to address this "new wave of eutrophication" (Beusen et al., 2015) through science and policy, success will stem from identifying the long-term cumulative effects of anthropogenic activity and disentangling present sources from historic anthropogenic activity (Le Moal et al., 2019), both of which were investigated in this study.

4.3. Alternate Explanations for altered profiles

Other events and phenomena can alter sedimentation rates beyond anthropogenic events and can act as confounding factors when attempting to extricate historical events recorded in the sediment. The sediment profiles reconstructed during this study captured episodic events beyond documented discharge events from the PG facility, which we hypothesize are attributable to storms or other anthropogenic activities. Large storm events can alter sedimentation and nutrient accumulation rates as observed in other estuaries (Joyse et al., 2023; Liu and Fearn, 2000; Morton et al., 2007; Radabaugh et al., 2020; Smith et al., 2009). The elevated sedimentation between 6 – 8 cm depth in both cores may be due to Hurricane Irma which made landfall in Florida in September of 2017. Historic releases from Piney Point have also been associated with past storms, where preexisting structural failures have forced the emergency discharge of wastewater to protect from broader infrastructure damage at the expense of the estuary. Infrastructure vulnerabilities such as storm-associated breaches are anticipated to increase in relation to climate change and sea-level rise, contributing to continued sustainability challenges (Bridges et al., 2021; Huddleston et al., 2022) further stressing the need to improve nutrient sustainability by incorporating a circular economy model that reduces waste and increases reuse (Bilal et al., 2023) while accelerating advanced wastewater treatment efforts and facility closures.

Beyond industrial activities, other anthropogenically-driven events can cause changes in downcore sediment profiles. Sediment delivery can increase 5 – 10 fold in areas impacted by human activities compared to undisturbed systems (Dearing and Jones, 2003), such as extensive tree clearing (Baskaran et al., 2014), increased urbanization and agricultural development (Brush, 1989; McCall et al., 1984; Vaalgamaa and Conley, 2008), and channel dredging (Erftemeijer et al., 2012). However, loading patterns of total suspended solids to Tampa Bay reflect watershed rainfall patterns (Janicki Environmental Inc, 2023), suggesting that these other anthropogenically-driven events may not have drastically altered the sediment profiles in more recent years. Since many of these events are contemporaneous, disentangling them can prove difficult and highlights the need for additional studies to improve the understanding of sediment sources and sinks in estuaries.

Other considerations when using ^{210}Pb as a time marker proxy include reconstructing estuarine nutrient accumulation rates based on local geology and defining the influence of submarine groundwater discharge (SGD). Tampa Bay has naturally high P concentrations (Carlson and Yarbro, 2006; Doyle et al., 1989) due to the phosphatic quartz in the region's karst bedrock (Edgar et al., 2001). The underlying limestone can undergo slow dissolution and release P to near-surface sediments via diffusion and SGD. Excess ^{210}Pb decreased logarithmically in the base portion of each core, and secular equilibrium between ^{226}Ra and total ^{210}Pb activity was achieved at Piney Point Creek and was approached at Bishop Harbor (full ^{210}Pb inventory was not captured). This suggests that there is minimal influence of SGD within the top half meter of the sediments at the sampling locations and further supports external P deposition from sources such as Piney Point, which loaded upwards of 130 tons of P into lower Tampa Bay during April 2021 (Janicki Environmental Inc, 2023; Fig. 3).

4.4. Potential for legacy nutrient resuspension and regeneration

Coastal systems and their associated ecosystem services are

vulnerable to storm disturbances, which have increased in severity and frequency with climate change (Paerl et al., 2018). Estuaries including Tampa Bay are susceptible to sediment resuspension driven by wind, waves, and storms, which subsequently influence benthic-pelagic coupling by stimulating a flux of bioavailable nutrients (e.g. NH_4^+, nitrate, and soluble reactive P [SRP]) into the water column (Corbett, 2010; Giffin and Corbett, 2003; Paerl et al., 2018; Porter et al., 2010; Schoellhamer, 1995; Smith and Caffrey, 2009; Sondergaard et al., 1992; Syvitski et al., 2022). As an example, water column nutrients (notably TKN and orthoP) doubled at two of the sites in this study following the passing of Hurricane Ian, a portion of which was likely resuspended from sediments (Giffin and Corbett, 2003; Paerl et al., 2018) or internally loaded from sediment diffusion as has been shown in other warm aquatic ecosystems (Fadum et al., 2023). This indicates that legacy nutrients have the potential to alter nutrient cycling long after episodic eutrophication events occur and therefore should be considered when managing estuaries and developing TMDLs with high anthropogenic activity in the surrounding watershed.

Resuspension events that promote benthic nutrient regeneration subsequently contribute to increased primary productivity where the balance between organic matter deposition and nutrient remineralization drives the fate and availability of nutrients in estuaries (Bianchi et al., 1999; DeMaster et al., 1985; McKee et al., 1983; Paerl et al., 2018; Twilley et al., 1999). Resuspended benthic nutrients can cause internal eutrophication events that alter water column nutrient stoichiometry, particularly in systems with high water residence time like Tampa Bay (Liu et al., 2024). Estuaries affected by cultural eutrophication can exhibit regime shifts where the dominant benthic community can transition from seagrass to phytoplankton-dominated communities (Phlips et al., 2021). Since phytoplankton are subject to high rates of decomposition, they can trigger positive feedback mechanisms that further increase nutrient availability (Chen et al., 2023; McGlathery et al., 2023; Valentine and Duffy, 2006).

In addition to storm-driven nutrient resuspension, legacy nutrients can be exchanged at the sediment–water interface through benthic nutrient regeneration. Based on the high P and N concentrations downcore at the sites coupled with previous studies conducted in Tampa Bay and similar estuaries, it is possible that nutrient regeneration in addition to storage can occur (Carlson and Yarbro, 2006; Dixon et al., 2014; Owens and Cornwell, 2012; Twilley et al., 1999). Desorption of P from minerals and organic matter can trigger SRP regeneration to the water column when conditions allow (e.g., supporting redox conditions, sediment type, high OC content, etc.; Liu et al., 2020; Patrick and Khalid, 1974; Twilley et al., 1999), which previous studies have observed in this estuary (Carlson and Yarbro, 2006; Owens and Cornwell, 2012). Recent work that incorporated field observations and precipitation/adsorption experiments found that when Piney Point wastewater was mixed with seawater, supersaturated conditions occurred (with respect to apatite) and promoted rapid precipitation of P to the sediments as insoluble apatite. This reaction minimized the impact of the discharge on water quality (relative to P) and limited its transport throughout the bay, although some migration of sedimentary P has been noted since 2021, likely due to physical transport (Major and Pasek, 2024). However, based on the increases in water column P and N that we observed after Hurricane Ian, additional work, such as *in situ* benthic flux studies and/or bioassays would be beneficial to confirm the mobility and fate of these nutrients, particularly relative to storm-induced resuspension. While these P forms may be identifiable with other advanced spectroscopic techniques, such as X-ray adsorption spectroscopy (Judy et al., 2021) and/or operationally defined P pools via sequential extractions (SEDEX; Anderson and Delaney, 2000; Ruttenberg, 1992), they are not identifiable via ^{31}P NMR, further supporting the absence of NMR-identifiable P compounds beyond orthoP and pyrophosphate found in this study. The regeneration of NH_4^+ from sediments following dense phytoplankton blooms was seen after the 2021 Piney Point discharge event near these study sites (Chen et al., 2023). This regeneration event was shortly followed by a HAB event dominated by *Karenia brevis*, a toxin-producing dinoflagellate responsible for red tide and extensive fish and marine mammal kills (Beck et al., 2022; Chen et al., 2023; Morrison et al., 2023). Future studies should include quantifying both benthic flux and redox profiles to further refine the understanding of the mechanisms driving nutrient regeneration and storage in estuarine sediments so they can be properly accounted for in nutrient budgets through a mass balance approach.

The unique depleted $\delta^{15}N$ signature of the Piney Point wastewater SPM (−17.88 ‰ ± 0.76) captured by Morrison et al. (2023) during the 2021 discharge event was not seen in these sediment profiles, presumably due to extensive microbial reworking and assimilation of ammonium by phytoplankton in the water column before being deposited to the benthos (Morrison et al., 2023; Robinson et al., 2012). In marine regions with high sediment accretion, $\delta^{15}N$ values of surface sediments are close to or equal to the $\delta^{15}N$ values of the sinking flux (Robinson et al., 2012), and typically increase ~ 2 ‰ during early burial, driven by many factors including oxygen exposure time, remineralization, and coupled nitrification–denitrification (Alkhatib et al., 2012; Robinson et al., 2012). The changes in $\delta^{13}C$ and $\delta^{15}N$ values downcore captured at these sites are likely a reflection of organic matter remineralization and benthic flux of NH_4^+ to the water column, reinforcing conclusions made by Chen et al. (2023). Further, these stable isotopes provide insight into the importance of benthic-pelagic coupling in estuaries like Tampa Bay, which are tightly linked and drive ecosystem stability (Crump et al., 2023).

4.5. Stoichiometric nutrient imbalances in sediments

Nutrient stoichiometry can also provide insights into aquatic ecosystem sustainability, as alterations in the forms and proportions of nutrients delivered to the coast can act as an additional stressor with nutrient load increases (Glibert, 2012). In particular, regional changes in stoichiometry can influence water quality and phytoplankton growth rates (Sterner and Elser, 2003). Most ecosystems have elevated N:P ratios globally due to extensive anthropogenic N sources, particularly from high atmospheric N deposition and agriculture practices. In some settings, P accumulates in soils and water bodies, decreasing N:P ratios (Yan et al., 2016), which was captured in this study. The N:P mass ratios in these estuarine sediments were consistently lower (0.08 ± 0.01 for Bishop Harbor and 5.06 ± 0.49 for Piney Point Creek) than average N:P ratios of major biospheric compartments (6 – 7 for open ocean, 7 for plankton, 7 – 10 for terrestrial soils; Penuelas et al., 2020; Wu et al., 2022) supporting previous work that has identified Tampa Bay as a N-limited estuary (Greening et al., 2014). These N:P ratios are most representative of fertilizer and sewage contributions and are comparable to sediments of eutrophic lakes (Sterner and Elser, 2003). Imbalanced N:P ratios such as these can lead to increased primary metabolism (Penuelas et al., 2020) and high planktonic growth rates (Sterner and Elser, 2003), heightening the potential for algae blooms and shifts in community composition over time (Miyazako et al., 2015). Shifts in nutrient stoichiometry can also affect phytoplankton metabolism, including the production of toxins leading to adverse effects on predator–prey interactions and ultimately disrupting ecosystem stability and functions (Glibert, 2012). Growing N:P imbalance will continue to have significant ecological implications on primary producers' structure, growth rate, and diversity (Penuelas et al., 2020; Peñuelas and Sardans, 2022; Sterner and Elser, 2003), hence why they are important to incorporate into aquatic studies.

Based on the downcore nutrient profiles and stoichiometric ratios coupled with water quality data following a high-magnitude hurricane, benthic nutrient regeneration and resuspension events may occur in these back bay regions of the estuary. Due to the long residence time and slow flushing rates of estuaries like Tampa Bay that are restricted at the mouth, it is possible that resuspended and regenerated nutrients could have long-term effects on water quality and ecosystem services while

exacerbating eutrophication. Moreover, regime shifts in primary producers have been documented to follow extensive eutrophication events in estuaries globally (Buskey et al., 2001; Conversi et al., 2015; Phlips et al., 2021). Alternative stable states may develop over time, however, ecosystem services often become suspended for significant lengths of time before some form of ecosystem rebound occurs, and sometimes the return state exhibits significant differences from the original state. By accounting for nutrient recycling and resuspension in estuarine nutrient budgets, degradation trajectories could be avoided in the future.

5. Conclusions

This study used the sediment record to quantify nutrient storage in back bay regions of Tampa Bay, Florida, and investigated the effects of episodic wastewater discharge events on sedimentation rates and nutrient stoichiometry. This was done with the consideration that Tampa Bay has a broad range of anthropogenic stressors in addition to the Piney Point phosphogypsum facility. The ^{210}Pb age-depth model used to establish deposition timeframes and sedimentation rates was coupled with independent chemical markers to validate periods of wastewater discharge, highlighting an alternative methodology when independent time markers (e.g., ^{137}Cesium) cannot be used to strengthen the model. The sediment and nutrient accumulation rates determined in this study show increased deposition and storage during wastewater discharge timeframes, stressing the influence of eutrophication events on legacy nutrients in coastal systems. Sediment nutrients were predominantly in the form of orthoP, NH_4^+, and organic N with imbalanced N:P ratios, which could influence water quality, biogeochemistry, and disrupt critical ecosystem services if resuspended or regenerated, however, additional studies such as benthic flux and/or bioassays experiments are recommended to confirm the mobility and fate of these legacy nutrients.

Globally, nutrients stored within the estuarine sediments are important pools to consider when establishing nutrient budgets and associated management strategies. They may contribute to internal nutrient loading and therefore can reinforce positive feedback cycles of estuarine eutrophication, which can induce HAB events, coastal hypoxia, and dead zones. Tampa Bay exhibits features similar to those of other estuarine settings globally and therefore, lessons learned from this study should be considered in other systems that have watersheds dominated by anthropogenic activity. Most National Estuary Programs develop nutrient reduction goals based on TMDLs that strictly incorporate external source loading. This study suggests that this approach could be overlooking legacy nutrients, which may be a major source contributor and need to be considered to achieve pollutant reduction targets to better protect coastal systems. Additionally, the effects of eutrophication will likely grow more complex and unpredictable as a result of climate change and sea-level rise. Integrating improved nutrient budgets with climate management plans may improve the resilience of estuaries facing interconnected and complex stressors in the future.

CRediT authorship contribution statement

Amanda R. Chappel: Writing – review & editing, Writing – original draft, Methodology, Investigation, Formal analysis, Data curation, Conceptualization. **William F. Kenney:** Writing – review & editing, Methodology, Formal analysis, Data curation. **Matthew N. Waters:** Writing – original draft, Conceptualization. **Caroline Buchanan Fisher:** Writing – review & editing, Methodology, Formal analysis, Data curation. **João H.F. Amaral:** Writing – review & editing, Investigation. **Edward J. Phlips:** Writing – review & editing, Funding acquisition. **Elise S. Morrison:** Writing – review & editing, Writing – original draft, Methodology, Funding acquisition, Formal analysis, Conceptualization.

Declaration of competing interest

The authors declare that they have no known competing financial interests or personal relationships that could have appeared to influence the work reported in this paper.

Acknowledgments

This project was supported by the National Science Foundation award CBET 2130675 to E. Morrison and Edward Phlips (University of Florida) and the Science and Technologies for Phosphorus Sustainability (STEPS) Center, a National Science Foundation Science and Technology Center (CBET-2019435). Many thanks to Todd Van Natta and Patrick Norby at the UF Center for Coastal Solutions (field operations), Jason Curtis at the UF Stable Isotope Laboratory (laboratory analysis), Shin-Ah Lee, Megan Sanford, Emily Watts, and Bobby Scharping, (field, laboratory, and data analysis assistance), and Thomas Bianchi, David Kaplan, and Andrew Altieri (insightful data discussions).

Appendix A. Supplementary data

Supplementary data to this article can be found online at https://doi.org/10.1016/j.ecolind.2025.113329.

Data availability

The datasets generated during and/or analyzed during the current study are available in Supplemental Information and from the corresponding author on reasonable request.

References

Alkhatib, M., Lehmann, M.F., Del Giorgio, P.A., 2012. The nitrogen isotope effect of benthic remineralization-nitrification-denitrification coupling in an estuarine environment. Biogeosciences 9, 1633–1646. https://doi.org/10.5194/bg-9-1633-2012.

Altieri, A.H., Gedan, K.B., 2015. Climate change and dead zones. Glob. Change Biol. 21, 1395–1406. https://doi.org/10.1111/gcb.12754.

Anderson, L.D., Delaney, M.L., 2000. Sequential extraction and analysis of phosphorus in marine sediments: Streamlining of the SEDEX procedure. Limnol. Oceanogr. 45, 509–515. https://doi.org/10.4319/lo.2000.45.2.0509.

Appleby, P.G., 2008. Three decades of dating recent sediments by fallout radionuclides: a review. The Holocene 18, 83–93. https://doi.org/10.1177/0959683607085598.

Appleby, P.G., Oldfield, F., 1978. The calculation of lead-210 dates assuming a constant rate of supply of unsupported ^{210}Pb to the sediment. Catena 5, 1–8. https://doi.org/10.1016/S0341-8162(78)80002-2.

Ardila, P.A.R., Alonso, R.Á., Valsero, J.J.D., García, R.M., Cabrera, F.Á., Cosío, E.L., Laforet, S.D., 2023. Assessment of heavy metal pollution in marine sediments from southwest of Mallorca island. Spain. Environ. Sci. Pollut. Res. 30, 16852–16866. https://doi.org/10.1007/s11356-022-25014-0.

Arias-Ortiz, A., Masqué, P., Garcia-Orellana, J., Serrano, O., Mazarrasa, I., Marbà, N., Lovelock, C.E., Lavery, P.S., Duarte, C.M., 2018. Reviews and syntheses: ^{210}Pb-derived sediment and carbon accumulation rates in vegetated coastal ecosystems – setting the record straight. Biogeosciences 15, 6791–6818. https://doi.org/10.5194/bg-15-6791-2018.

Baskaran, M., Coleman, C.H., Santschi, P.H., 1993. Atmospheric depositional fluxes of ^{7}Be and ^{210}Pb at Galveston and College Station. Texas. J. Geophys. Res. Atmospheres 98, 20555–20571. https://doi.org/10.1029/93JD02182.

Baskaran, M., Nix, J., Kuyper, C., Karunakara, N., 2014. Problems with the dating of sediment core using excess ^{210}Pb in a freshwater system impacted by large scale watershed changes. J. Environ. Radioact. 138, 355–363. https://doi.org/10.1016/j.jenvrad.2014.07.006.

Baskaran, M., Swarzenski, P.W., 2007. Seasonal variations on the residence times and partitioning of short-lived radionuclides (^{234}Th, ^{7}Be and ^{210}Pb) and depositional fluxes of ^{7}Be and ^{210}Pb in Tampa Bay. Florida. Mar. Chem. 104, 27–42. https://doi.org/10.1016/j.marchem.2006.06.012.

Beck, M.W., Altieri, A., Angelini, C., Burke, M.C., Chen, J., Chin, D.W., Gardiner, J., Hu, C., Hubbard, K.A., Liu, Y., Lopez, C., Medina, M., Morrison, E., Phlips, E.J., Raulerson, G.E., Scolaro, S., Sherwood, E.T., Tomasko, D., Weisberg, R.H., Whalen, J., 2022. Initial estuarine response to inorganic nutrient inputs from a legacy mining facility adjacent to Tampa Bay. Florida. Mar. Pollut. Bull. 178, 113598. https://doi.org/10.1016/j.marpolbul.2022.113598.

Beck, M.W., Cressman, K., Griffin, C., Caffrey, J., 2018. Water Quality Trends Following Anomalous Phosphorus Inputs to Grand Bay, Mississippi, USA. Gulf Caribb. Res. 1–14. https://doi.org/10.18785/gcr.2901.02.

Bianchi, T.S., Pennock, J.R., Twilley, R.R. (Eds.), 1999. Biogeochemistry of Gulf of Mexico Estuaries. Wiley, New York Weinheim.
Bilal, E., Bellefqih, H., Bourgier, V., Mazouz, H., Dumitraş, D.-G., Bard, F., Laborde, M., Caspar, J.P., Guilhot, B., Iatan, E.-L., Bounakhla, M., Iancu, M.A., Marincea, Ş., Essakhraoui, M., Li, B., Diwa, R.R., Ramirez, J.D., Chernysh, Y., Chubur, V., Roubík, H., Schmidt, H., Beniazza, R., Cánovas, C.R., Nieto, J.M., Haneklaus, N., 2023. Phosphogypsum circular economy considerations: A critical review from more than 65 storage sites worldwide. J. Clean. Prod. 414, 137561. https://doi.org/10.1016/j.jclepro.2023.137561.
Bouargane, B., Laaboubi, K., Biyoune, M.G., Bakiz, B., Atbir, A., 2023. Effective and innovative procedures to use phosphogypsum waste in different application domains: review of the environmental, economic challenges and life cycle assessment. J. Mater. Cycles Waste Manag. 25, 1288–1308. https://doi.org/10.1007/s10163-023-01617-8.
Brenner, M., Schelske, C.L., Kenney, W.F., 2004. Inputs of dissolved and particulate ^{226}Ra to lakes and implications for ^{210}Pb dating recent sediments. J. Paleolimnol. 32, 53–66. https://doi.org/10.1023/B:JOPL.0000025281.54969.03.
Bridges, T., King, J., Simm, J., Beck, M., Collins, G., Lodder, Q., Mohan, R., 2021. International Guidelines on Natural and Nature-Based Features for Flood Risk Management. Engineer Research and Development Center (U.S.). https://hdl.handle.net/11681/41946.
Brush, G.S., 1989. Rates and patterns of estuarine sediment accumulation. Limnol. Oceanogr. 34, 1235–1246. https://doi.org/10.4319/lo.1989.34.7.1235.
Bucci, L., Alaka, L., Hagen, A., Delgado, S., Beven, J., 2023. National Hurricane Center Tropical Cyclone Report. Hurricane Ian No AL092022. https://www.nhc.noaa.gov/data/tcr/AL092022_Ian.pdf.
Beusen, A.H.W., Bouwman, A.F., Beek, L.P.H., Mogollón, J.M., Middelburg, J.J., 2015. Global riverine N and P transport to ocean increased during the twentieth century despite increased retention along the aquatic continuum. Biogeosciences. https://doi.org/10.5194/bgd-12-20123-2015.
Buchanan Fisher, C., Vardanyan, L., Judy, J., In Review. Spectroscopic Investigation of the Speciation of Phosphorus Forms Entering and Leaving Everglades Stormwater Treatment Areas. J. Env. Quality.
Burnett, W.C., Elzerman, A.W., 2001. Nuclide migration and the environmental radiochemistry of Florida phosphogypsum. J. Environ. Radioact. 54, 27–51. https://doi.org/10.1016/S0265-931X(00)00164-8.
Buskey, E.J., Liu, H., Collumb, C., Bersano, J.G.F., 2001. The Decline and Recovery of a Persistent Texas Brown Tide Algal Bloom in the Laguna Madre (Texas, USA). Estuaries 24, 337. https://doi.org/10.2307/1353236.
Cade-Menun, B., 2005. Characterizing phosphorus in environmental and agricultural samples by ^{31}P nuclear magnetic resonance spectroscopy. Talanta 66, 359–371. https://doi.org/10.1016/j.talanta.2004.12.024.
Cade-Menun, B., Liu, C.W., 2014. Solution Phosphorus-31 Nuclear Magnetic Resonance Spectroscopy of Soils from 2005 to 2013: A Review of Sample Preparation and Experimental Parameters. Soil Sci. Soc. Am. J. 78, 19–37. https://doi.org/10.2136/sssaj2013.05.0187dgs.
Carlson, P., Yarbro, L., 2006. Benthic Oxygen and Nutrient Fluxes in Tampa. In: Bay: A Final Report to the Tampa Bay Estuary Program. Florida Department of Environmental Protection, and U.S. Environmental Protection Agency Gulf of Mexico Program. Technical Publication # 04-06. Florida Fish and Wildlife Research Institute. https://drive.google.com/file/d/1TMD6jB2uCDYlV7-yoqan5L8m5rEU0VzZ/view.
Carpenter, S.R., Bennett, E.M., 2011. Reconsideration of the planetary boundary for phosphorus. Environ. Res. Lett. 6, 014009. https://doi.org/10.1088/1748-9326/6/1/014009.
Cheesman A.W. Rocca J. Turner B.L. Phosphorus Characterization in Wetland Soils by Solution Phosphorus-31 Nuclear Magnetic Resonance Spectroscopy DeLaune R.D. Reddy K.R. Richardson C.J. Megonigal J.P. SSSA book series 2015 American Society of Agronomy and Soil Science Society of America Madison, WI, USA 639 665. https://doi.org/10.2136/sssabookser10.c33.
Cheesman, A.W., Turner, B.L., Reddy, K.R., 2014. Forms of organic phosphorus in wetland soils. Biogeosciences 11, 6697–6710. https://doi.org/10.5194/bg-11-6697-2014.
Chen, J., Weisberg, R.H., Liu, Y., Zheng, L., 2018. The Tampa Bay Coastal Ocean Model Performance for Hurricane Irma. Mar. Technol. Soc. J. 52, 33–42. https://doi.org/10.4031/MTSJ.52.3.6.
Chen, J., Weisberg, R.H., Liu, Y., Zheng, L., Zhu, J., 2019. On the Momentum Balance of Tampa Bay. J. Geophys. Res. Oceans 124, 4492–4510. https://doi.org/10.1029/2018JC014890.
Chen, Y., Li, M., Glibert, P.M., Heil, C., 2023. Mu*r*Ky waters: Modeling the succession from r to K strategists (diatoms to dinoflagellates) following a nutrient release from a mining facility in Florida. Limnol. Oceanogr. 68, 2288–2304. https://doi.org/10.1002/lno.12420.
Conversi, A., Dakos, V., Gårdmark, A., Ling, S., Folke, C., Mumby, P.J., Greene, C., Edwards, M., Blenckner, T., Casini, M., Pershing, A., Möllmann, C., 2015. A holistic view of marine regime shifts. Philos. Trans. r. Soc. B Biol. Sci. 370, 20130279. https://doi.org/10.1098/rstb.2013.0279.
Corbett, D.R., 2010. Resuspension and estuarine nutrient cycling: insights from the Neuse River Estuary. Biogeosciences 7, 3289–3300. https://doi.org/10.5194/bg-7-3289-2010.
Crump, B.C., Testa, J.M., Dunton, K.H., 2023. Estuarine Ecology, Third ed. Wiley, Hoboken NJ.
Curtis, J.H., Hodell, D.A., Brenner, M., 1996. Climate Variability on the Yucatan Peninsula (Mexico) during the Past 3500 Years, and Implications for Maya Cultural Evolution. Quat. Res. 46, 37–47. https://doi.org/10.1006/qres.1996.0042.
Da, F., Friedrichs, M.A.M., St-Laurent, P., 2018. Impacts of Atmospheric Nitrogen Deposition and Coastal Nitrogen Fluxes on Oxygen Concentrations in Chesapeake Bay. J. Geophys. Res. Oceans 123, 5004–5025. https://doi.org/10.1029/2018JC014009.
DeAngelis, B., Sutton-Grier, A., Colden, A., Arkema, K., Baillie, C., Bennett, R., Benoit, J., Blitch, S., Chatwin, A., Dausman, A., Gittman, R., Greening, H., Henkel, J., Houge, R., Howard, R., Hughes, A., Lowe, J., Scyphers, S., Sherwood, E., Westby, S., Grabowski, J., 2020. Social Factors Key to Landscape-Scale Coastal Restoration: Lessons Learned from Three U.S. Case Studies. Sustainability 12, 869. https://doi.org/10.3390/su12030869.
Dearing, J.A., Jones, R.T., 2003. Coupling temporal and spatial dimensions of global sediment flux through lake and marine sediment records. Glob. Planet. Change 39, 147–168. https://doi.org/10.1016/S0921-8181(03)00022-5.
Defforey, D., Cade-Menun, B.J., Paytan, A., 2017. A new solution ^{31}P NMR sample preparation scheme for marine sediments. Limnol. Oceanogr. Methods 15, 381–393. https://doi.org/10.1002/lom3.10166.
Dellapenna, T.M., Hoelscher, C., Hill, L., Al Mukaimi, M.E., Knap, A., 2020. How tropical cyclone flooding caused erosion and dispersal of mercury-contaminated sediment in an urban estuary: The impact of Hurricane Harvey on Buffalo Bayou and the San Jacinto Estuary, Galveston Bay, USA. Sci. Total Environ. 748, 141226. https://doi.org/10.1016/j.scitotenv.2020.141226.
Dellapenna, T.M., Kuehl, S.A., Schaffner, L.C., 1998. Sea-bed Mixing and Particle Residence Times in Biologically and Physically Dominated Estuarine Systems: a Comparison of Lower Chesapeake Bay and the York River Subestuary. Estuar. Coast. Shelf Sci. 46, 777–795. https://doi.org/10.1006/ecss.1997.0316.
DeMaster, D.J., McKee, B.A., Nittrouer, C.A., Jiangchu, Q., Guodong, C., 1985. Rates of sediment accumulation and particle reworking based on radiochemical measurements from continental shelf deposits in the East China Sea. Cont. Shelf Res. 4, 143–158. https://doi.org/10.1016/0278-4343(85)90026-3.
Diaz, R.J., Rosenberg, R., 2008. Spreading Dead Zones and Consequences for Marine Ecosystems. Science 321, 926–929. https://doi.org/10.1126/science:1156401.
Dixon, L.K., Murphy, P.J., Becker, N.M., Charniga, C.M., 2014. The potential role of benthic nutrient flux in support of Karenia blooms in west Florida (USA) estuaries and the nearshore Gulf of Mexico. Harmful Algae 38, 30–39. https://doi.org/10.1016/j.hal.2014.04.005.
Doyle, L.J., Brooks, G.R., Fanning, K.A., Van Vleet, E.S., Byrne, R.H., Blake, N.J.. A characterization of Tampa Bay sediments. https://digitalcommons.usf.edu/basgp_report/108.
Edgar, T., Yates, K., Brooks, G., Cronin, Hollander, D., Runnels, R., Sutton, P., Werzinski, Y., Willard, D., 2001. Tampa Bay Integrated Science Pilot Study Historical and Prehistorical Record of Tampa Bay Environments., USGS Numbered Series.
Elser, J., Bennett, E., 2011. A broken biogeochemical cycle. Nature 478, 29–31. https://doi.org/10.1038/478029a.
Engstrom, D.R., Schottler, S.P., Leavitt, P.R., Havens, K.E., 2006. A Reevaluation Of The Cultural Eutrophication Of Lake Okeechobee Using Multiproxy Sediment Records. Ecol. Appl. 16, 1194–1206. https://doi.org/10.1890/1051-0761(2006)016[1194:AROTCE]2.0.CO;2.
Erftemeijer, P.L.A., Riegl, B., Hoeksema, B.W., Todd, P.A., 2012. Environmental impacts of dredging and other sediment disturbances on corals: A review. Mar. Pollut. Bull. 64, 1737–1765. https://doi.org/10.1016/j.marpolbul.2012.05.008.
Fadum, J.M., Waters, M.N., Hall, E.K., 2023. Trophic state resilience to hurricane disturbance of Lake Yojoa. Honduras. Sci. Rep. 13, 5681. https://doi.org/10.1038/s41598-023-32712-3.
Fisher, M.M., Brenner, M., Reddy, K.R., 1992. A simple, inexpensive piston corer for collecting undisturbed sediment/water interface profiles. J. Paleolimnol. 157–161. https://doi.org/10.1016/S0302-3524(82)80069-8.
Foucher, A., Chaboche, P.-A., Sabatier, P., Evrard, O., 2021. Global review of 137Cs and 210Pbxs fallout used for dating sediment cores. https://doi.org/10.1594/PANGAEA.931493.
Garrett, M., Wolny, J., Truby, E., Heil, C., Kovach, C., 2011. Harmful algal bloom species and phosphate-processing effluent: Field and laboratory studies. Mar. Pollut. Bull. 62, 596–601. https://doi.org/10.1016/j.marpolbul.2010.11.017.
Giffin, D., Corbett, D.R., 2003. Evaluation of sediment dynamics in coastal systems via short-lived radioisotopes. J. Mar. Syst. 42, 83–96. https://doi.org/10.1016/S0924-7963(03)00068-X.
Glibert, P.M., 2012. Ecological stoichiometry and its implications for aquatic ecosystem sustainability. Curr. Opin. Environ. Sustain. 4, 272–277. https://doi.org/10.1016/j.cosust.2012.05.009.
Goldberg E.D. Geochronology with lead-210, radioactive dating, IAEA 1963 , in: International Atomic Energy Contributions 1510. Vienna, p. 21.
Graustein, W.C., Turekian, K.K., 1986. ^{210}Pb and ^{137}Cs in air and soils measure the rate and vertical profile of aerosol scavenging. J. Geophys. Res. Atmospheres 91, 14355–14366. https://doi.org/10.1029/JD091iD13p14355.
Greening, H., Janicki, A., Sherwood, E.T., Pribble, R., Johansson, J.O.R., 2014. Ecosystem responses to long-term nutrient management in an urban estuary: Tampa Bay, Florida, USA. Estuar. Coast. Shelf Sci. 151, A1–A16. https://doi.org/10.1016/j.ecss.2014.10.003.
Gwynn, J.P., Hatje, V., Casacuberta, N., Sarin, M., Osvath, I., 2024. The effect of climate change on sources of radionuclides to the marine environment. Commun. Earth Environ. 5, 135. https://doi.org/10.1038/s43247-024-01241-w.
Harris, D., Horwáth, W.R., Van Kessel, C., 2001. Acid fumigation of soils to remove carbonates prior to total organic carbon or CARBON-13 isotopic analysis. Soil Sci. Soc. Am. J. 65, 1853–1856. https://doi.org/10.2136/sssaj2001.1853.
Heidarzadeh, M., Iwamoto, T., Šepić, J., Mulia, I.E., 2023. Normal and reverse storm surges along the coast of Florida during the September 2022 Hurricane Ian:

Observations, analysis, and modelling. Ocean Model 185, 102250. https://doi.org/10.1016/j.ocemod.2023.102250.
Henderson, C.S., 2004. Piney Point Phosphate Plant. An Environmental Analysis. https://digitalcommons.usf.edu/cgi/viewcontent.cgiarticle=1062&context=honorstheses.
Huddleston, P., Smith, T., White, I., Elrick-Barr, C., 2022. Adapting critical infrastructure to climate change: A scoping review. Environ. Sci. Policy 135, 67–76. https://doi.org/10.1016/j.envsci.2022.04.015.
Jani, J., Yang, Y.-Y., Lusk, M.G., Toor, G.S., 2020. Composition of nitrogen in urban residential stormwater runoff: Concentrations, loads, and source characterization of nitrate and organic nitrogen. PLoS One 15, e0229715. https://doi.org/10.1371/journal.pone.0229715.
Janicki Environmental Inc, 2023. Estimates of total nitrogen, total phosphorus, total suspended solids, and biochemical oxygen demand loadings to Tampa Bay, Florida: 2017–2021 (No. TBEP 7229). Tampa Bay Nitrogen Management Consortium. URL: https://drive.google.com/file/d/1KARuSC5fGx05MuT1wiOQFWNXysBokkQl/view. Google Drive.
Javaruski, J., Adhikari, P.L., Muller, J., Parsons, M.L., 2022. Preservation of brevetoxins in Southwest Florida coastal sediments. Harmful Algae 114, 102222. https://doi.org/10.1016/j.hal.2022.102222.
Joyse, K.M., Khan, N.S., Moyer, R.P., Radabaugh, K.R., Hong, I., Chappel, A.R., Walker, J.S., Sanders, C.J., Engelhart, S.E., Kopp, R.E., Horton, B.P., 2023. The characteristics and preservation potential of Hurricane Irma's overwash deposit in southern Florida, USA. Mar. Geol. 461, 107077. https://doi.org/10.1016/j.margeo.2023.107077.
Judy, J.D., Harris, W., Hettiarachchi, G.M., Buchanan, A.C., Reddy, K.R., 2021. Mineralogy of particulate inputs and P-speciation and mineralogy of recently accreted soils within Everglades stormwater treatment wetlands. Sci. Total Environ. 781, 146740. https://doi.org/10.1016/j.scitotenv.2021.146740.
Kahle, D., Wickham, H., 2013. ggmap: Spatial Visualization with ggplot2. R J 5, 144–161. https://journal.r-project.org/archive/2013-1/kahle-wickham.pdf.
Kaste, J.M., Volante, P., Elmore, A.J., 2021. Bomb ^{137}Cs in modern honey reveals a regional soil control on pollutant cycling by plants. Nat. Commun. 12, 1937. https://doi.org/10.1038/s41467-021-22081-8.
Kenney, W.F., Schelske, C.L., Chapman, A.D., 2001. Changes in polyphosphate sedimentation: a response to excessive phosphorus enrichment in a hypereutrophic lake. Can. J. Fish. Aquat. Sci. 58, 879–887. https://doi.org/10.1139/f01-040.
Kenney, W.F., Shields, M.R., Bianchi, T.S., Kolker, A.S., Mohrig, D., 2022. Excess ^{210}Pb as an indicator of flood-stage sediments in prograding, Wax Lake Delta, USA. Mar. Geol. 453, 106914. https://doi.org/10.1016/j.margeo.2022.106914.
Krishnaswamy, S., Lal, D., Martin, J.M., Meybeck, M., 1971. Geochronology of lake sediments. Earth Planet. Sci. Lett. 11, 407–414. https://doi.org/10.1016/0012-821X(71)90202-0.
Lamb, A.L., Wilson, G.P., Leng, M.J., 2006. A review of coastal palaeoclimate and relative sea-level reconstructions using δ13C and C/N ratios in organic material. Earth-Sci. Rev. 75, 29–57. https://doi.org/10.1016/j.earscirev.2005.10.003.
Larson, R., Schwing, P., Guzman, C., Rivera, D., Wischmeyer, D., Murray, J., Brooks, G., 2023. Assessing the benthic impacts of the piney point discharge. Fla. Sci. 86, 35–49. https://www.jstor.org/stable/27265794.
Last, W.M., Smol, J.P., Birks, H.J.B., 2001. Tracking Environmental Change Using Lake Sediments. Kluwer Academic Publishers, Dordrecht.
Le Moal, M., Gascuel-Odoux, C., Ménesguen, A., Souchon, Y., Étrillard, C., Levain, A., Moatar, F., Pannard, A., Souchu, P., Lefebvre, A., Pinay, G., 2019. Eutrophication: A new wine in an old bottle? Sci. Total Environ. 651, 1–11. https://doi.org/10.1016/j.scitotenv.2018.09.139.
Lebo, M.E., Paerl, H.W., Peierls, B.L., 2012. Evaluation of Progress in Achieving TMDL Mandated Nitrogen Reductions in the Neuse River Basin, North Carolina. Environ. Manage. 49, 253–266. https://doi.org/10.1007/s00267-011-9774-5.
Li, W., Joshi, S.R., Hou, G., Burdige, D.J., Sparks, D.L., Jaisi, D.P., 2015. Characterizing Phosphorus Speciation of Chesapeake Bay Sediments Using Chemical Extraction, ^{31}P NMR, and X-ray Absorption Fine Structure Spectroscopy. Environ. Sci. Technol. 49, 203–211. https://doi.org/10.1021/es504648d.
Lin, P., Klump, J.V., Guo, L., 2024. Chemical speciation, reactivity, and long-term burial of sedimentary phosphorus in Green Bay, a seasonally hypoxia-influenced freshwater estuary. Sci. Total Environ. 174957. https://doi.org/10.1016/j.scitotenv.2024.174957.
Liu, J., Krom, M.D., Ran, X., Zang, J., Liu, J., Yao, Q., Yu, Z., 2020. Sedimentary phosphorus cycling and budget in the seasonally hypoxic coastal area of Changjiang Estuary. Sci. Total Environ. 713, 136389. https://doi.org/10.1016/j.scitotenv.2019.136389.
Liu, K., Fearn, M.L., 2000. Reconstruction of Prehistoric Landfall Frequencies of Catastrophic Hurricanes in Northwestern Florida from Lake Sediment Records. Quat. Res. 54, 238–245. https://doi.org/10.1006/qres.2000.2166.
Liu, Y., Weisberg, R.H., Zheng, L., Sun, Y., Chen, J., Law, J.A., Hu, C., Cannizzaro, J.P., Frazer, T.K., 2024. A tracer model nowcast/forecast study of the Tampa Bay, Piney Point effluent plume: Rapid response to an environmental hazard. Mar. Pollut. Bull. 198, 115840. https://doi.org/10.1016/j.marpolbul.2023.115840.
Major, J.D., Pasek, M.A., 2024. Constraining the mineralogy and mobility of phosphate resulting from the Piney Point wastewater dump. Florida Department of Protection Technical Report. https://floridadep.gov/oeat/oeat/documents/constraining-mineralogy-and-mobility-phosphate-resulting-piney-point-wastewater.
Makarov, M.I., Haumaier, L., Zech, W., 2002. Nature of soil organic phosphorus: an assessment of peak assignments in the diester region of ^{31}P NMR spectra. Soil Biol. Biochem. 34, 1467–1477. https://doi.org/10.1016/S0038-0717(02)00091-3.
Malone, T.C., Newton, A., 2020. The Globalization of Cultural Eutrophication in the Coastal Ocean: Causes and Consequences. Front. Mar. Sci. 7, 670. https://doi.org/10.3389/fmars.2020.00670.
McCall, P.L., Robbins, J.A., Matisoff, G., 1984. ^{137}Cs and ^{210}Pb transport and geochronologies in urbanized reservoirs with rapidly increasing sedimentation rates. Chem. Geol. 44, 33–65. https://doi.org/10.1016/0009-2541(84)90066-4.
McGlathery, K.J., Sundback, K., Fong, P., Aoki, L., Anderson, I., (Eds.), 2023. Estuarine Benthic Algae, In: Estuarine Ecology, John Wiley & Sons, Inc. pp. 181–212.
McKee, B.A., Nittrouer, C.A., DeMaster, D.J., 1983. Concepts of sediment deposition and accumulation applied to the continental shelf near the mouth of the Yangtze River. Geology 11, 631–633. https://doi.org/10.1130/0091-7613(1983)11<631:COSDAA>2.0.CO;2.
McLaren, T.I., Smernik, R.J., McLaughlin, M.J., McBeath, T.M., Kirby, J.K., Simpson, R.J., Guppy, C.N., Doolette, A.L., Richardson, A.E., 2015. Complex Forms of Soil Organic Phosphorus–A Major Component of Soil Phosphorus. Environ. Sci. Technol. 49, 13238–13245. https://doi.org/10.1021/acs.est.5b02948.
Miyazako, T., Kamiya, H., Godo, T., Koyama, Y., Nakashima, Y., Sato, S., Kishi, M., Fujihara, A., Tabayashi, Y., Yamamuro, M., 2015. Long-term trends in nitrogen and phosphorus concentrations in the Hii River as influenced by atmospheric deposition from East Asia: East Asian atmospheric N and P deposition. Limnol. Oceanogr. 60, 629–640. https://doi.org/10.1002/lno.10051.
Morrison, E.S., Phlips, E., Badylak, S., Chappel, A.R., Altieri, A.H., Osborne, T.Z., Tomasko, D., Beck, M.W., Sherwood, E., 2023. The response of Tampa Bay to a legacy mining nutrient release in the year following the event. Front. Ecol. Evol. 11, 1144778. https://doi.org/10.3389/fevo.2023.1144778.
Morton, R.A., Gelfenbaum, G., Jaffe, B.E., 2007. Physical criteria for distinguishing sandy tsunami and storm deposits using modern examples. Sediment. Geol. 200, 184–207. https://doi.org/10.1016/j.sedgeo.2007.01.003.
Niemitz, J., Haynes, C., Lasher, G., 2013. Legacy sediments and historic land use: Chemostratigraphic evidence for excess nutrient and heavy metal sources and remobilization. Geology 41, 47–50. https://doi.org/10.1130/G33547.1.
Owens, M., Cornwell, J., 2012. Tampa Bay Sediment Nutrient Fluxes–Final Report Technical Report# 08-12. https://drive.google.com/file/d/1U3MvEUXgzHOfSH_Cf7otfaEz2IsJf86U/view.
Paerl, H.W., Crosswell, J.R., Van Dam, B., Hall, N.S., Rossignol, K.L., Osburn, C.L., Hounshell, A.G., Sloup, R.S., Harding, L.W., 2018. Two decades of tropical cyclone impacts on North Carolina's estuarine carbon, nutrient and phytoplankton dynamics: implications for biogeochemical cycling and water quality in a stormier world. Biogeochemistry 141, 307–332. https://doi.org/10.1007/s10533-018-0438-x.
Patrick, W.H., Khalid, R.A., 1974. Phosphate Release and Sorption by Soils and Sediments: Effect of Aerobic and Anaerobic Conditions. Science 186, 53–55. https://doi.org/10.1126/science:186.4158.53.
Penuelas, J., Janssens, I.A., Ciais, P., Obersteiner, M., Sardans, J., 2020. Anthropogenic global shifts in biospheric N and P concentrations and ratios and their impacts on biodiversity, ecosystem productivity, food security, and human health. Glob. Change Biol. 26, 1962–1985. https://doi.org/10.1111/gcb.14981.
Peñuelas, J., Sardans, J., 2022. The global nitrogen-phosphorus imbalance. Science 375, 266–267. https://doi.org/10.1126/science:abl4827.
Pérez-López, R., Macías, F., Cánovas, C.R., Sarmiento, A.M., Pérez-Moreno, S.M., 2016. Pollutant flows from a phosphogypsum disposal area to an estuarine environment: An insight from geochemical signatures. Sci. Total Environ. 553, 42–51. https://doi.org/10.1016/j.scitotenv.2016.02.070.
Phlips, E.J., Badylak, S., Nelson, N.G., Hall, L.M., Jacoby, C.A., Lasi, M.A., Lockwood, J.C., Miller, J.D., 2021. Cyclical Patterns and a Regime Shift in the Character of Phytoplankton Blooms in a Restricted Sub-Tropical Lagoon, Indian River Lagoon, Florida. United States. Front. Mar. Sci. 8, 730934. https://doi.org/10.3389/fmars.2021.730934.
Porter, E., Mason, R., Sanford, L., 2010. Effect of tidal resuspension on benthic–pelagic coupling in an experimental ecosystem study. Mar. Ecol. Prog. Ser. 413, 33–53. https://doi.org/10.3354/meps08709.
Qin, X., Cao, Y., Guan, H., Hu, Q., Liu, Z., Xu, J., Hu, B., Zhang, Z., Luo, R., 2023. Resource utilization and development of phosphogypsum-based materials in civil engineering. J. Clean. Prod. 387, 135858. https://doi.org/10.1016/j.jclepro.2023.135858.
R Core Team, 2022. A language and environment for statistical computing 2022. https://www.R-project.org.
Radabaugh, K.R., Moyer, R.P., Chappel, A.R., Dontis, E.E., Russo, C.E., Joyse, K.M., Bownik, M.W., Goeckner, A.H., Khan, N.S., 2020. Mangrove Damage, Delayed Mortality, and Early Recovery Following Hurricane Irma at Two Landfall Sites in Southwest Florida, USA. Estuaries Coasts 43, 1104–1118. https://doi.org/10.1007/s12237-019-00564-8.
Rangel-Buitrago, N., Rizzo, A., Neal, W.J., Mastronuzzi, G., 2023. Sediment pollution in coastal and marine environments. Mar. Pollut. Bull. 192, 115023. https://doi.org/10.1016/j.marpolbul.2023.115023.
Reddy, K.R., Vardanyan, L., Hu, J., Villapando, O., Bhomia, R.K., Smith, T., Harris, W.G., Newman, S., 2020. Soil phosphorus forms and storage in stormwater treatment areas of the Everglades: Influence of vegetation and nutrient loading. Sci. Total Environ. 725, 138442. https://doi.org/10.1016/j.scitotenv.2020.138442.
Robbins, J.A., Holmes, C., Halley, R., Bothner, M., Shinn, E., Graney, J., Keeler, G., tenBrink, M., Orlandini, K.A., Rudnick, D., 2000. Time-averaged fluxes of lead and fallout radionuclides to sediments in Florida Bay. J. Geophys. Res. Oceans 105, 28805–28821. https://doi.org/10.1029/1999JC000271.
Robinson, R.S., Kienast, M., Luiza Albuquerque, A., Altabet, M., Contreras, S., De Pol Holz, R., Dubois, N., Francois, R., Galbraith, E., Hsu, T., Ivanochko, T., Jaccard, S., Kao, S., Kiefer, T., Kienast, S., Lehmann, M., Martinez, P., McCarthy, M., Möbius, J., Pedersen, T., Quan, T.M., Ryabenko, E., Schmittner, A., Schneider, R., Schneider-

Mor, A., Shigemitsu, M., Sinclair, D., Somes, C., Studer, A., Thunell, R., Yang, J., 2012. A review of nitrogen isotopic alteration in marine sediments. Paleoceanography 27, 2012PA002321. https://doi.org/10.1029/2012PA002321.
Robledo Ardila, P.A., Álvarez-Alonso, R., Árcega-Cabrera, F., Durán Valsero, J.J., Morales García, R., Lamas-Cosío, E., Oceguera-Vargas, I., DelValls, A., 2024. Assessment and Review of Heavy Metals Pollution in Sediments of the Mediterranean Sea. Appl. Sci. 14, 1435. https://doi.org/10.3390/app14041435.
Rodgers, K., McLellan, I., Peshkur, T., Williams, R., Tonner, R., Knapp, C.W., Henriquez, F.L., Hursthouse, A.S., 2020. The legacy of industrial pollution in estuarine sediments: spatial and temporal variability implications for ecosystem stress. Environ. Geochem. Health 42, 1057–1068. https://doi.org/10.1007/s10653-019-00316-4.
Rutherford, P.M., Dudas, M.J., Samek, R.A., 1994. Environmental impacts of phosphogypsum. Sci. Total Environ. 149, 1–38. https://doi.org/10.1016/0048-9697(94)90002-7.
Ruttenberg, K.C., 1992. Development of a sequential extraction method for different forms of phosphorus in marine sediments. Limnol. Oceanogr. 37, 1460–1482. https://doi.org/10.4319/lo.1992.37.7.1460.
Schelske, C.L., Peplow, A., Brenner, M., Spencer, C.N., 1994. Low-background gamma counting: applications for ^{210}Pb dating of sediments. J. Paleolimnol. 10, 115–128. https://doi.org/10.1007/BF00682508.
Schelske, C.L., Robbins, J.A., Gardner, W.S., Conley, D.J., Bourbonniere, R.A., 1988. Sediment Record of Biogeochemical Responses to Anthropogenic Perturbations of Nutrient Cycles in Lake Ontario. Can. J. Fish. Aquat. Sci. 45, 1291–1303. https://doi.org/10.1139/f88-151.
Schoellhamer, D.H., 1995. Sediment Resuspension Mechanisms in Old Tampa Bay. Florida. Estuar. Coast. Shelf Sci. 40, 603–620. https://doi.org/10.1006/ecss.1995.0041.
Scolaro, S., Beck, M.W., Burke, M.C., Raulerson, G.E., Sherwood, E.T., 2023. Piney Point, seagrass, and macroalgae: impact assessment and a case for enhanced macroalgae monitoring. Fla. Sci. 86, 339–345. https://www.researchgate.net/profile/Marcus-Beck-3/publication/373524462_Piney_Point_seagrass_and_macroalgae_impact_assessment_and_a_case_for_enhanced_macroalgae_monitoring/links/64f07bb2c40f1d22df7c1774/Piney-Point-seagrass-and-macroalgae-impact-assessment-and-a-case-for-enhanced-macroalgae-monitoring.pdf.
Silva, L.F.O., Oliveira, M.L.S., Crissien, T.J., Santosh, M., Bolivar, J., Shao, L., Dotto, G.L., Gasparotto, J., Schindler, M., 2022. A review on the environmental impact of phosphogypsum and potential health impacts through the release of nanoparticles. Chemosphere 286, 131513. https://doi.org/10.1016/j.chemosphere.2021.131513.
Smith, K.A., Caffrey, J.M., 2009. The effects of human activities and extreme meteorological events on sediment nitrogen dynamics in an urban estuary, Escambia Bay, Florida, USA. Hydrobiologia 627, 67–85. https://doi.org/10.1007/s10750-009-9716-x.
Smith, T.J., Anderson, G.H., Balentine, K., Tiling, G., Ward, G.A., Whelan, K.R.T., 2009. Cumulative impacts of hurricanes on Florida mangrove ecosystems: Sediment deposition, storm surges and vegetation. Wetlands 29, 24–34. https://doi.org/10.1672/08-40.1.
Smith, V.H., 1998. Cultural Eutrophication of Inland, Estuarine, and Coastal Waters. In: Pace, M.L., Groffman, P.M. (Eds.), Successes, Limitations, and Frontiers in Ecosystem Science. Springer, New York, New York, NY, pp. 7–49. https://doi.org/10.1007/978-1-4612-1724-4_2.
Smoak, J.M., Breithaupt, J.L., Smith, T.J., Sanders, C.J., 2013. Sediment accretion and organic carbon burial relative to sea-level rise and storm events in two mangrove forests in Everglades National Park. Catena 104, 58–66. https://doi.org/10.1016/j.catena.2012.10.009.
Sondergaard, M., Kristensen, P., Jeppesen, E., 1992. Phosphorus release from resuspended sediment in the shallow and wind-exposed Lake Arreso, Denmark. Hydrobiologia 228, 91–99. https://doi.org/10.1007/BF00006480.
Sterner, R.W., Elser, J.J., 2003. Ecological Stoichiometry: The Biology of Elements from Molecules to the Biosphere. Princeton University Press. https://doi.org/10.1515/9781400885695.
Swarzenski, P.W., Orem, W.H., McPherson, B.F., Baskaran, M., Wan, Y., 2006. Biogeochemical transport in the Loxahatchee River estuary, Florida: The role of submarine groundwater discharge. Mar. Chem. 101, 248–265. https://doi.org/10.1016/j.marchem.2006.03.007.
Swarzenski, P.W., Porcelli, D., Andersson, P., Smoak, J., 2003. The Behavior of U- and Th-series Nuclides in the Estuarine Environment. Rev. Mineral. Geochem. 52, 577–606. https://doi.org/10.2113/0520577.
SFWMD, Reddy, R., Bianchi, T., LeMeur, M., Morrison, E.S., Vardanyan, L., Rocca, J., Liu, Y., 2017. Identification and Quantification of Organic Phosphorus Forms in the Water Column and Soils of the Everglades Stormwater Treatment Areas (STAs). UF Collaborative Research Initiative Science for the Everglades Stormwater Treatment Areas (CRESTA) No. 4600003031-WO02.
Switzer, T.S., Tyler-Jedlund, A.J., Rogers, K.R., Grier, H., Jr, R.H.M., Fox, S., 2011. Nekton response to discharged PO_4 process H_2O (Technical). Florida Fish and Wildlife Conservation Commission, Fish and Wildlife Research Institute. http://hdl.handle.net/1834/41127.
Syvitski, J., Ángel, J.R., Saito, Y., Overeem, I., Vörösmarty, C.J., Wang, H., Olago, D., 2022. Earth's sediment cycle during the Anthropocene. Nat. Rev. Earth Environ. 3, 179–196. https://doi.org/10.1038/s43017-021-00253-w.
Törnquist, P., Eriksson, M., Olszewski, G., Carlsson, M., López-Lora, M., Pettersson, H.B. L., 2023. On the use of dated sediments to investigate historical nuclear discharges. Mar. Pollut. Bull. 188, 114637. https://doi.org/10.1016/j.marpolbul.2023.114637.
Turner, B.L., Mahieu, N., Condron, L.M., 2003. Phosphorus-31 Nuclear Magnetic Resonance Spectral Assignments of Phosphorus Compounds in Soil NaOH–EDTA Extracts. Soil Sci. Soc. Am. J. 67, 497–510. https://doi.org/10.2136/sssaj2003.4970.
Twilley, R.R., Cowan, J., Miller-Way, T., Montagna, P.A., Mortazavi, B., 1999. Benthic Nutrient Fluxes in Selected Estuaries in the Gulf of Mexico. In: Biogeochemistry of Gulf of Mexico Estuaries. John Wiley & Sons Inc, pp. 163–209.
Vaalgamaa, S., Conley, D.J., 2008. Detecting environmental change in estuaries: Nutrient and heavy metal distributions in sediment cores in estuaries from the Gulf of Finland. Baltic Sea. Estuar. Coast. Shelf Sci. 76, 45–56. https://doi.org/10.1016/j.ecss.2007.06.007.
Valentine, J.F., Duffy, J.E. (Eds.), 2006. The Central Role of Grazing in seagrass ecology. Seagrasses: biology, ecology, conservation. Springer, Dordrecht, pp. 463–501.
Waters, M.N., Kenney, W.F., Brenner, M., Webster, B.C., 2019. Organic carbon sequestration in sediments of subtropical Florida lakes. PLoS One 14, e0226273. https://doi.org/10.1371/journal.pone.0226273.
Watson, S.J., Cade-Menun, B.J., Needoba, J.A., Peterson, T.D., 2018. Phosphorus Forms in Sediments of a River-Dominated Estuary. Front. Mar. Sci. 5, 302. https://doi.org/10.3389/fmars.2018.00302.
Wickham, H., 2016. Ggplot2: elegant graphics for data analysis. https://ggplot2.tidyverse.org.
Wickham, H., Averick, M., Bryan, J., Chang, W., McGowan, L., François, R., Grolemund, G., Hayes, A., Henry, L., Hester, J., Kuhn, M., Pedersen, T., Miller, E., Bache, S., Müller, K., Ooms, J., Robinson, D., Seidel, D., Spinu, V., Takahashi, K., Vaughan, D., Wilke, C., Woo, K., Yutani, H., 2019. Welcome to the Tidyverse. J. Open Source Softw. 4, 1686. https://doi.org/10.21105/joss.01686.
Wu, Z., Li, J., Sun, Y., Peñuelas, J., Huang, J., Sardans, J., Jiang, Q., Finlay, J.C., Britten, G.L., Follows, M.J., Gao, W., Qin, B., Ni, J., Huo, S., Liu, Y., 2022. Imbalance of global nutrient cycles exacerbated by the greater retention of phosphorus over nitrogen in lakes. Nat. Geosci. 15, 464–468. https://doi.org/10.1038/s41561-022-00958-7.
Xu, D., Ding, S., Li, B., Jia, F., He, X., Zhang, C., 2012. Characterization and optimization of the preparation procedure for solution P-31 NMR analysis of organic phosphorus in sediments. J. Soils Sediments 12, 909–920. https://doi.org/10.1007/s11368-012-0510-4.
Yan, Z., Han, W., Peñuelas, J., Sardans, J., Elser, J.J., Du, E., Reich, P.B., Fang, J., 2016. Phosphorus accumulates faster than nitrogen globally in freshwater ecosystems under anthropogenic impacts. Ecol. Lett. 19, 1237–1246. https://doi.org/10.1111/ele.12658.
Zhou, S., Margenot, A.J., 2023. Muddied Waters: The Use of "Residual" And "Legacy" Phosphorus. Environ. Sci. Technol. 57, 21535–21539. https://doi.org/10.1021/acs.est.3c04733.
Zielinski, R.A., Al-Hwaiti, M.S., Budahn, J.R., Ranville, J.F., 2011. Radionuclides, trace elements, and radium residence in phosphogypsum of Jordan. Environ. Geochem. Health 33, 149–165. https://doi.org/10.1007/s10653-010-9328-4.